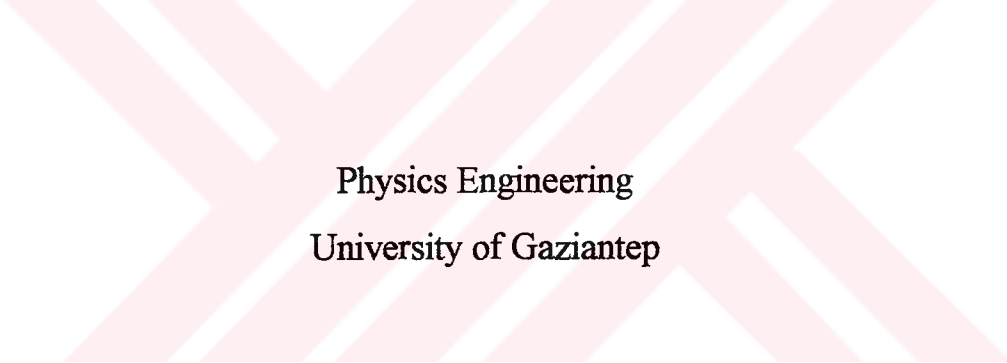


TRANSIENT PHOTOCONDUCTIVITY AND PHOTOLUMINESCENCE IN WIDE-  
BAND GAP CRYSTALS UNDER GENERATION OF RADIATION DEFECT DUE  
TO MULTIPHOTON ABSORPTION OF LASER RADIATION

77709

Ph. D. THESIS

in



Physics Engineering  
University of Gaziantep

By

R. Güler (ÖZKAN) YILDIRIM

August 1998

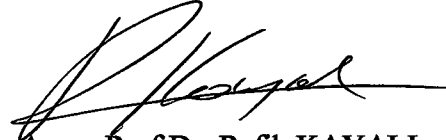
Approval of the Graduate School of Natural and Applied Science.



Assoc.Prof.Dr. Ali Rıza TEKİN

**Director**

I certify that I have read this thesis and that in my opinion it is fully adequate, in scope and quality, as a dissertation for the degree of Doctor of Philosophy.



Assoc.Prof.Dr. Refik KAYALI

**Chairman of the Department**

I certify that I have read this thesis and that in my opinion it is fully adequate, in scope and quality, as a dissertation for the degree of Doctor of Philosophy.



Prof.Dr. Meral HOŞCAN

**Supervisor**

**Examining Committee in Charge**

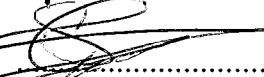
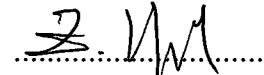
Prof.Dr.Zehra YEĞİNGİL

Prof.Dr. Meral HOŞCAN

Prof.Dr.Sadettin ÖZYAZICI

Assoc.Prof.Dr. Ramazan ESEN

Assist.Prof.Dr. Ramazan KOÇ



## ABSTRACT

### TRANSIENT PHOTOCONDUCTIVITY AND PHOTOLUMINESCENCE IN WIDE-BAND GAP CRYSTALS UNDER GENERATION OF RADIATION DEFECT DUE TO MULTIPHOTON ABSORPTION OF LASER RADIATION

YILDIRIM (ÖZKAN) Rabia Güler

Ph.D. in Physics Engineering

Supervisor: Prof.Dr. Meral HOŞCAN

August 1998, 83 pages

Four-photon excitation of valance electrons to the conduction band is needed for the calculation of prebreakdown energy deposition in NaCl at 532 nm. Since NaCl has band energy of 8.6 eV and laser pulse at 532 nm has energy 2.33 eV, the four-photon absorption is the primary absorption process in NaCl.

There are two main theories about the lattice heating resulting from the absorption of photons by electrons in the conduction band. The first one is the polaron

model and second one is the avalanche theory of free electron generation. It should be mentioned that each model is based on several theories.

In this study, we : have used multiphoton-polaron-defect model and multiphoton-assisted-avalanche model; in multiphoton-polaron defect model, hole absorption , direct e-h recombination, and polaron absorption contribute to heating, with other species contributing much less. In the second model, due to heating the crystal may be damaged.

We have solved the kinetic equations with computer simulation to find the concentration of primary defects such as  $V_K$ -centers, F-center, ionized F-center, and free electron and hole densities.

**Keywords:** Prebreakdown energy absorption, laser, alkali halides, primary defects.



## ÖZET

# LASER RADYASYONU ETKİSİ İLE ÇOKLUFOTON YUTULMASINDAN DOLAYI OLUŞAN RADYASYON HASARLARININ SONUCUNDA GENİŞ BAND ARALIĞINA SAHİP KRİSTALLERDEKİ FOTOLUMİNESANS VE FOTOİLETKENLİK GEÇİŞLERİ

YILDIRIM (ÖZKAN) Rabia Güler

Doktora Tezi

Gaziantep Üniversitesi Fizik Mühendisliği Bölümü

Tez Danışmanı: Prof.Dr. Meral HOŞCAN

Agustos 1998, 83 sayfa

532 nm de, NaCl kristalindeki önyıkınım enerji birikiminin hesaplamasında elektronların valans banddan iletkenlik bandına geçmesi için dört foton ile uyarılması gerekir. NaCl'nin enerji band aralığı 8.6 eV ve 532 nm deki laser pulsunun enerjisi 2.33 eV tur. Bu nedenle dört foton soğurulması NaCl için temel soğurma işlemidir.

İletkenlik bandındaki elektronların foton soğurması ile kristalde oluşan ısınma hakkında iki temel teori vardır. Birincisi polaron model, ikincisi serbest elektron oluşumunun çık teorisisidir. Her iki model çeşitli teoriler üzerine kurulduğu belirtilmelidir.

İletkenlik bandındaki elektronların foton soğurması ile kristalde oluşan ısınma hakkında iki temel teori vardır. Birincisi polaron model, ikincisi serbest elektron oluşumunun çığ teorisidir. Her iki model çeşitli teoriler üzerine kurulduğu belirtilmelidir.

Bu çalışmada çoklufoton-polaron-kusur ve çoklufoton destekli çığ modelini kullandık; çoklufoton-polaron-kusur modelinde yalnız deşik soğurulması, doğrudan e-h birleşmesi ve polaron soğurulması ısınmaya katkıda bulunurlar; diğer kusur çeşitleri daha az katkıda bulunurlar. İkinci modelde ısınmadan dolayı kristal hasara uğrayabilir.

$V_K$ - merkezleri, F-merkezi, iyonlaşmış F-merkezi, serbest elektron ve deşik yoğunlukları gibi temel kusurlarını bulmak için kinetik denklemleri bilgisayar uyarlaması ile çözdük.

Anahtar Kelimeler: Önyıkınım enerji yutulması, lazer, alkali halide, temel kusurlar.

## ACKNOWLEDGEMENTS

The author would like to express her sincerest gratitude and thanks to her supervisor Prof. Dr. Meral HOŞCAN for her guidance, encouragement, assistance, advice, suggestions in the course of this work, and above all, for her warm friendship.

She would like to thank to Assist. Prof. Dr. Zihni ÖZTÜRK, Assist. Prof. Dr. Ramazan KOÇ for their helping.

Special thanks are due to her parents and husband for their patience.

This thesis dedicated to her child Bedirhan.

# TABLE OF CONTENTS

<b>ABSTRACT</b>	<b>iii</b>
<b>ÖZET</b>	<b>iv</b>
<b>ACKNOWLEDGEMENT</b>	<b>vi</b>
<b>TABLE OF CONTENTS</b>	<b>viii</b>
<b>LIST OF TABLES</b>	<b>xi</b>
<b>LIST OF FIGURES</b>	<b>xii</b>
<b>LIST OF SYMBOLS</b>	<b>xv</b>
<b>1. INTRODUCTION</b>	<b>1</b>
<b>2. LITERATURE SURVEY</b>	<b>3</b>
<b>3. THEORY</b>	<b>12</b>
3.1 The Physical Properties of Crystals	12
3.1.1 Alkali Halide (Ionic Crystals)	12
3.1.2 Energy Band	14
3.1.3 Alkali Halide Imperfection	16
3.1.4 Production of Color Centers	17
3.1.5 Definition of Laser Damage and Mechanism of Valance	18
Electron Excitation	
3.2 Color Centers	21
3.2.1 Electron Centers	21
3.2.2 Hole Trapping Centers	23



3.3 The Characteristic of the F-Band Absorption	26
3.4 Configuration Co-ordinate Diagrams	29
3.5 Electrical Properties of Crystals Containing Defects	32
3.5.1 Photoconductivity	32
<b>4. MICROSCOPIC PROCESS OF CRYSTAL-PHOTON INTERACTION</b>	<b>35</b>
4.1 Introduction	35
4.2 Electron-Hole Pair Generation, Primary Defect Production and Secondary Energy Absorption	37
4.2.1 Four-Photon Electron-Hole (e-h) Pair Generation	37
4.2.2 Avalanche Generation and Free Carrier Heating	38
4.2.3 Polaron Heating	41
4.2.4 Primary Defects	42
4.3 Parameters of the Primary Defect Model	46
4.4 Model Equations	48
<b>5. THE STUDY AND THE THEORETICAL PROCEDURE</b>	<b>55</b>
5.1 Introduction	55
<b>6. RESULT AND CONCLUSION</b>	<b>69</b>
<b>LIST OF REFERENCES</b>	<b>72</b>
<b>APPENDIX</b>	<b>76</b>
<b>CURRICULUM VITAE</b>	<b>82</b>

## LIST OF TABLES

Table 1	Wavelengths of the Absorption Peaks Arising from Various Trapped-Electron and Trapped-Hole Centers in Alkali Halide.	30
Table 2	Kinetic Equations.	52
Table 3	Definition and Parameters in Table 2.	53



## LIST OF FIGURES

Figure 3.1	The structure of the NaCl-type alkali halide.	13
Figure 3.2	Energy band diagram for an insulator.	14
Figure 3.3	Energy band with some energy levels.	15
Figure 3.4	The various point defects that can exist in a crystal.	17
Figure 3.5	The formation of a) a Schottky defect b) a Frenkel defect.	18
Figure 3.6	Common color centers in alkali halides $MX$ . These include electron-excess centers, notably the F center and related defects (the F' center has an extra electron; the $F_A$ center is an F center with an adjacent cation impurity; the $F_2$ center is two adjacent F centers), and two centers involving $X_2^-$ molecular ions, namely, the self-trapped hole ( $V_K$ center) and neutral anion interstitial (H center).	24
Figure 3.7	Models of color centers from Schulman and Compton. The H, $V_1$ and centers have tetrahedral symmetry; the $V_2$ , $V_3$ and other centers have cubic symmetry.	27
Figure 3.8	Atomic structure of the $V_K$ center.	28
Figure 3.9	Configuration coordinate diagram ( $A \rightarrow B$ ) absorption, ( $C \rightarrow D$ ) emission for a defect center.	33
Figure 4.1	Composite double-logarithmic plot of temperature increase at focal point vs incident energy of 532 nm pulses.	38
Figure 4.2	Schematic energy level diagram of the $V_K$ center and STE [9]. The orbitals are the molecular levels occupied by the eleven outer atomic chlorine p-electrons in the self-trapped hole or $V_K$ center configuration.	45

( $Cl_2$ ). The excited electron of the STE occupies either state  $^1\Sigma_u^+(S_1)$  or  $^3\Sigma_u^+(S_3)$  when trapped from the conduction band. Recombination with the hole from either state results in the luminescence labeled  $\sigma$  and  $\pi$  respectively, forms the dissociative  $^1\Sigma_g^+$  STE  $\sigma_u \rightarrow \sigma_g$  hole transition (electron:  $\sigma_g \rightarrow \sigma_u$ ).

Figure 4.3	Free-carrier density [9].	51
Figure 5.1	Free carrier density, in terms of the density of active atoms, $N = 2.2 \times 10^{22} \text{ cm}^{-3}$ (for polaron model).	57
Figure 5.2	Free hole density in terms of the density of active atoms, $N = 2.2 \times 10^{22} \text{ cm}^{-3}$ (for polaron model).	58
Figure 5.3	Density of $V_{K1}$ -centers in terms of the density of active atoms, $N = 2.2 \times 10^{22} \text{ cm}^{-3}$ (for polaron model).	58
Figure 5.4	Density of $V_{K2}$ -centers in terms of the density of active atoms, $N = 2.2 \times 10^{22} \text{ cm}^{-3}$ (for polaron model).	59
Figure 5.5	Density of $V_{K3}$ -centers in terms of the density of active atoms, $N = 2.2 \times 10^{22} \text{ cm}^{-3}$ (for polaron model).	59
Figure 5.6	Density of STEs in excited state $S^*$ in terms of the density of active atoms, $N = 2.2 \times 10^{22} \text{ cm}^{-3}$ (for polaron model).	60
Figure 5.7	Density of STEs in excited state $S_1$ in terms of the density of active atoms, $N = 2.2 \times 10^{22} \text{ cm}^{-3}$ (for polaron model).	60
Figure 5.8	Density of STEs in excited state $S_3$ in terms of the density of active atoms, $N = 2.2 \times 10^{22} \text{ cm}^{-3}$ (for polaron model).	61
Figure 5.9	Density of F-centers in terms of the density of active atoms, $N = 2.2 \times 10^{22} \text{ cm}^{-3}$ (for polaron model).	61
Figure 5.10	Density of ionized $F'$ -centers in terms of the density of active atoms, $N = 2.2 \times 10^{22} \text{ cm}^{-3}$ (for polaron model).	62
Figure 5.11	Free carrier density with $\sigma^{(4)} = 2 \times 10^{-113} \text{ cm}^8 \text{ sec}^3$ , dashed line for $F_p = 1.343 \text{ photons/cm}^3 \text{ sec}$ , broken line for $F_p = 5.343 \text{ photons/cm}^3 \text{ sec}$ ,	62

solid line for  $F_p = 7.343$  photons/cm<sup>3</sup>sec

Figure 5.12 Free carrier density with  $\sigma^{(4)} = 3 \times 10^{-113}$  cm<sup>8</sup>sec<sup>3</sup>, dashed line for  $F_p = 1.343$  photons/cm<sup>3</sup>sec, broken line for  $F_p = 5.343$  photons/cm<sup>3</sup>sec, solid line for  $F_p = 7.343$  photons/cm<sup>3</sup>sec 63

Figure 5.13 Density of free carrier, with multiphoton-assisted-avalanche model 63

Figure 5.14 Density of free holes, with multiphoton-assisted-avalanche model 65

Figure 5.15 Density of  $V_{K1}$ , with multiphoton-assisted-avalanche model 66

Figure 5.16 Density of  $V_{K2}$ , with multiphoton-assisted-avalanche model 66

Figure 5.17 Density of  $V_{K3}$ , with multiphoton-assisted-avalanche model 67

Figure 5.18 Density of  $S^*$ , with multiphoton-assisted-avalanche model 67

Figure 5.19 Density of  $S_1$ , with multiphoton-assisted-avalanche model 68

Figure 5.20 Density of  $S_3$ , with multiphoton-assisted-avalanche model 68

Figure 5.21 Density of  $n_F$ , with multiphoton-assisted-avalanche model 69

Figure 5.22 Density of  $n_{F'}$ , with multiphoton-assisted-avalanche model 69

## LIST OF SYMBOLS

CB	: Conduction Band
VB	: Valance Band
$n_c$	: Conduction Band Free Carrier
$p$	: Free holes
$V_{K1}$	: $V_{K1}$ - center
$V_{K2}$	: $V_{K2}$ - center
$V_{K3}$	: $V_{K3}$ - center
STE	: Self-Trapped-Exciton
$S^*$	: State of $S^*$ STE
$S_1$	: State of $S_1$ STE
$S_3$	: State of $S_3$ STE
$n_F$	: Density of F-center
$n_{F^*}$	: Density of ionized F-center
$N$	: Density of chlorine atom
e-h	: Electron hole pair

# CHAPTER 1

## INTRODUCTION

Color centers in solids have been studied intensively for nearly a century, not only because of their intrinsic interest but also because of the insight this study has given into the imperfection- determined properties of insulating solids.

A nominally transparent, wide band gap solid may be rendered an absorber when exposed to laser light of sufficiently high intensity. Interest in this subject of investigation is usually related to laser induced damage of optically components and theoretical and experimental investigations of this economically and technically important phenomenon have been continued in earnest since the early 1970's[1,2]. The mechanism(s) of induced absorption and damage are generally held to depend on the relative size of the laser photon energy  $\hbar\omega$ , and the material band gap,  $E_g$ . For  $\hbar\omega/E_g \ll 1$ , laser damage is attributed to avalanche ionization and subsequent Joule heating of the lattice through interaction of free carriers with the strong electric fields ( $10^6$  - $10^7$  V/cm) of the laser pulse in 1978 [3].

Aim of this study was to compute simulate the intrinsic behavior of NaCl in order to find the concentration of primary defects such as F-, V<sub>K</sub>- center, self trapped excitons (STE), conduction band carrier concentration, free--hole density.

In this study we have used multiphoton-polaron-defect heating and multiphoton-assisted-avalanche heating model. The four-photon crossection used were  $\sigma^{(4)} = 2 \times 10^{-113} \text{ cm}^8 \text{ sec}^3$  and  $\sigma^{(4)} = 3 \times 10^{-113} \text{ cm}^8 \text{ sec}^3$  for multiphoton-polaron-defect heating and  $\sigma^{(4)} = 1.5 \times 10^{-114} \text{ cm}^8 \text{ sec}^3$  for multiphoton- assisted-avalanche heating model. The laser pulse was expressed as  $F(t) = F_p \exp\{-[(t/\tau) - \sqrt{5}]^2\}$ , the calculation begins at  $t=0$  and the pulse peaks at  $t=190$  psec for  $\tau=85$  psec.

This thesis consists of six chapters which are organised in such a way that, in the second chapter, comprehensive literature survey of research on the subject is summarized. In the third chapter, theory of wide-band gap is presented. Microscopic processes of crystal-photon interaction is presented in chapter four. In chapter five the solution of kinetic equation are given. Results and conclusion of this study are presented in chapter six.



## CHAPTER 2

### LITERATURE SURVEY

The existence of the colored specimens of normally colorless minerals has been known for much longer than a century and has been excited the curiosity of mineralogists, chemists and physicists. For example, natural rock salt crystal are known which are colored yellow because they selectively absorb blue light. Beginning with the early 1800's sporadic studies appear in the literature concerning the bleaching of these coloration, the thermoluminescence which sometimes accompanies it, and the reproduction of these coloration by electric sparks, ultraviolet light, high-energy corpuscular radiation, and by chemical means. In the early part of this century the attention of Przibam at Vienna, 1924, was attracted to the problem, and from him and his collaborators have come an extensive series of researches on the coloration and luminescence of solids, with particular emphasis on natural minerals Pohl at Göttingen, 1937, became interested in the conduction of electricity in insulating solids and through this was led into a study of the coloration of the alkali halides. The phenomena involved in the coloration were soon recognized to be of general importance for the understanding of electronic processes in solids.

From time to time more or less specific models of the color centers had been proposed by various investigators but critical experiments to establish the validity of these models were not and are not easy to devise with the recognition of the highly important influence of structural imperfections on the physical properties of solids, it seemed clear that imperfections were involved in the production and constitution of the color centers. As early as 1937 Boer proposed a model for one of the color centers in the alkali halides (the "F Center"), which consisted essentially of an electron trapped at the position of a missing halogen ion (halogen ion vacancy). Specific models of other color centers in the alkali halides were later proposed principally by Seitz, which likewise involved electrons or electron-deficiencies ("Positive hole") trapped at aggregates of positive and negative ion vacancies.

The mechanism of formation of color centers and their annihilation or transformation into other color centers have been under studied from the earliest history of the subject. Kinetic studies as is often the case in other fields, have not yielded a definitive picture of these processes, but current work along this line is more promising. Electronic and mass transport properties in solids are of course highly important in clarifying the above mechanism.

The effect of chemical impurities on the ease of coloration and on the nature of the color centers formed were also among the earliest observations in the study of the coloration of inorganic solids. Because of the often remarkable effects of these impurities there is considerable interest in the properties of impurity-doped crystals. For the same reason increased attention is currently being given to the very careful purification of the salts under investigation. The advantages has been taken of the marked effects of the impurities to enhance or depress the formation of various color centers or to create new coloration characteristic of the impurity addition.

When photon energy is a significant fraction of the band gap multiphoton absorption by valence band electrons may either contribute to the free carrier generation or be the dominant mechanism of free carrier production. The probability of simultaneous absorption of  $m$  photons, where  $m \geq \hbar \omega / E_g \geq m-1$ , drops precipitously with increasing order  $m$ , and the order of nonlinear absorption,  $m$ , for which multiphoton absorption becomes important to laser damage is not precisely known.

Proponents of the avalanche theory predict that two-photon absorption is probably the primary mechanism of damage [1], but deficiencies in the avalanche theory led Braunlich et al., in 1979[4-6] to propose that multiphoton absorption contributes to or is primarily responsible for damage in alkali halides for the cases where the band gap is bridged by 3, 4 or 5 photons ( $m = 3,4,5$ ).

Although not important as materials for high power laser components, alkali halides are primary materials for theoretical and experimental studies of laser-induced breakdown because they offer an extremely wide transparency region (for wavelengths of almost all laser  $10.5 \geq \lambda \geq 0.4 \mu\text{m}$ ) and, thus, laser frequency dependence of breakdown can be studied. In addition, a large data base of optical properties exists for these materials. NaCl is the prototype alkali halide in dielectric breakdown studies for historical reasons[1-3].

According to Smith [3] no direct proof of laser induced electron avalanche has been obtained for alkali halides and there also exists a lack of accurate values for critical parameters (for example multiphoton absorption cross sections) used in theoretical damage calculations. Experimental evidence supporting theories of laser damage lies in the laser frequency and pulse width dependence of the so-called damage threshold, which is the maximum intensity or electric field strength of a laser pulse that just causes damage. While the frequency- and pulse width-dependence of the damage threshold in alkali halides appears to be consistent with the avalanche model for  $m \geq 5$  [3,7] insufficient and contradictory data exist for  $m = 4$  NaCl ( $E_g = 8.6 \text{ eV}$ ,  $\hbar \omega = 2.33 \text{ eV}$ ) [3,7,8] to unequivocally assign damage to the avalanche mechanism. Thus it is important to

measure energy absorption prior to damage to determine whether the avalanche mechanism is operative in this case, since measurement of the damage threshold is inconclusive. Attainment of this goal requires use of a technique highly sensitive to small absorbed energies arising from high energy pulses, a simple direct attenuation experiment is insufficiently sensitive for high order absorption processes.

Jones et al. in 1988[9], are to report the successful measurement of calibrated pre-breakdown energy deposition in NaCl exposed to intense pulses of 532 nm (photon energy 2.33 eV) laser light, using the photoacoustic technique. The primary process is shown to be valance electron excitation via four- photon absorption. The photoacoustic technique was suggested for possible use in pre-breakdown absorption measurements by Brawer[10] and was previously used by Horn[11] to obtain the three-photon absorption cross section at 1.06  $\mu\text{m}$  in TlBr and TlClBr.

The cross section for simultaneous absorption of four photons by valance band electrons in NaCl is obtained by Jones[9] experimentally. This information was to be used in model calculations of laser damage thresholds at 532 nm wavelength for this material.

Recent successes in obtaining the cross sections for three-photon absorption in thallium halides by Horn et al. in 1985,[11] using the photoacoustic technique, and in potassium iodide by Brost et al. in 1984,[12] exploiting electron-hole recombination luminescence, indicated one or both of these methods might yield the four-photon cross section,  $\sigma^{(4)}$ , in NaCl. Both experiments are rather simple in principle. In the *photoacoustic technique* conversion of the absorbed electromagnetic energy to heat results in local expansion of the material and generation of sound wave. All that is required to obtain a signal is to conduct the sound wave to an acoustic transducer. In the *luminescence method* it is necessary to collect emitted photons resulting from electron-hole (e-h) recombination. In both models demonstration of the nonlinear order of the excitation; i.e. the number of photons absorbed by valance in the primary excitation process, is given by the dependence of the signal on the incident laser pulse energy.

In series of classical experiments performed at the Naval Research Laboratories and Japan in the 1970's Kabler et al.,[13] and later Suzuki and Hirai[14] have demonstrated that primary defect such as  $V_k^-$ ,  $F^-$ , H- centers and self trapped excitons are produced extremely rapidly and efficiently from multiphoton or impact generated excitons in alkali halides and alkaline earth halides[15]. The formation of primary defect centers, all of which are strong absorbers of photons in the UV to IR of the electromagnetic spectrum, were suspected by Williams's and Kabler to seriously affect the mechanism by which, according to the basic damage theories, energy from an intense photon beam is deposited to the lattice of these solids.

R.T. Williams and Kabler[16], the low lying states of self- trapped excitons STE's in alkali halide have been studied extensively by means of the luminescence emitted during electron- hole recombination. These investigations have shown that the metastable self- trapped configuration in which the luminescence originates consists of an electron bound to a hole which is itself localized on a pair of nearest- neighbor halide ions. The hole configuration is equivalent to the well-known stable  $X_2^-$  or  $V_k^-$ -center. The recombination luminescence spectra consists of broad bands, some of which are  $\sigma$  polarized, short-lived, and due to the decay of singlet excited states, and others which are  $\pi$  polarized, relatively long-lived, and due to triplet states.

A response of alkali halide crystals to the generation of electron- hole pairs is the formation of such primary defects as  $V_k$ , F- and H- centers, and self- trapped excitons. Upon excitation of an electron to the conduction band, the hole becomes localized in a covalent bond between two adjacent halide ions [17-19] to form a  $V_k^-$  center.

In many simple halide crystals, the lattice itself is not stable upon creation of electron- hole pairs. The generation of permanent defects in alkali halides is a classic problem of radiation damage and of solid-state photochemistry, but the striking interplay between electronic and nuclear degrees of freedom is not completely understood. In

1964, Plooley and Hersh, indicated that the self-trapped exciton (STE) as a progenitor of the F-center [20].

The mechanisms responsible for laser damage in transparent crystals are not entirely understood [21]. It is a widely accepted notation that breakdown in the near IR and visible is due to avalanche ionization [8]. An alternative is the multiphoton absorption model [5], which relies on multiphoton-generated free carriers in the conduction band [5] and valance band [22].

P. Horn et al. in 1983, [23] studied to several alkali halides. Several alkali halides have shown high susceptibility to point defect formation under proper irradiation by picosecond and nanosecond laser pulses. Such color centers, if formed during passage of the mode-locked pulse train through their samples, would consistute an inadmissible change in the initial sample condition for every pulse arriving later. They used X-ray irradiation to check for color center formation in thallium halides. Contrary to effects seen in alkali halides and earth alkaline halides, they found negligible point defect production in thallium halides even at extreme X-ray exposures. Free carrier are known to relax very quickly into color center precursors in alkali halides.

Dneprovskii et al., [24] observed five-photon absorption in NaCl using a ruby laser and measuring the induced photoconductivity. Aseev et al., [25] used the same measurements technique for a series of alkali halides exposed to laser pulses emitted by Nd and ruby lasers. They observed four-photon absorption in NaCl, KCl and NaBr under ruby illumination, five-photon absorption in NaBr and six-photon absorption in NaCl, KCl and KBr under Nd excitation. These results do not all make sense in terms of excitation across the band gap since, the 8.6 eV band gap of NaCl can not be bridged by six Nd photons (total energy 7 eV). Excitation to free-exciton states or impurities may have played a role.

Catalano et al.,[26] measured four-and five-photon absorption cross sections by way of the nonlinear photoconductivity technique using a Q-switched ruby laser in KBr, KI, KCl, and NaCl. Their results are:

$$\begin{aligned}\sigma^{(4)}(\text{KBr}) &= 2 \times 10^{-114} \text{ cm}^8 \text{ sec}^3 \\ \sigma^{(4)}(\text{KI}) &= (2 \pm 0.8) \times 10^{-114} \text{ cm}^8 \text{ sec}^3 \\ \sigma^{(5)}(\text{KCl}) &= (2.4 \pm 1.2) \times 10^{-140} \text{ cm}^{10} \text{ sec}^4 \\ \sigma^{(5)}(\text{NaCl}) &= (1.8 \pm 0.9) \times 10^{-140} \text{ cm}^{10} \text{ sec}^4\end{aligned}$$

However, these results have been severely criticized and considered invalid by Williams et al.,[27]. Assumptions made by Catalano et al., regarding the free carrier lifetimes ( $\approx 1\mu$  sec) were proven to be almost wrong (Williams et al., measured carrier density dependent lifetimes of 10 psec- 10 nsec).

Although these results do not include  $\sigma^{(4)}$  for NaCl, the values for KI or KBr could be used for multiphoton damage modeling if it was felt they reliable. Jones et al., [9] results (however, insofar as Catalano give a range for  $\sigma^{(4)}$ ) are in agreement with Catalano et al., in a range for  $\sigma^{(4)}$ .

Chen et al. in 1981,[28], studied solution of the kinetic equation governing trap filling consequences concerning dose dependence and dose-rate effects and they found an important result to emerge from the analysis is the depend of thermoluminescence output on the dose rate for a constant total dose.

Gorshkov et al., [29], measured the frequency and temperature dependence of the laser-induced breakdown thresholds of a number of alkali halides crystals. In the samples with the highest thresholds the dependence agree qualitative with the avalanche ionization theory and this mechanism is the probable cause of their destruction.



The role of laser-induced primary defect formation in optical breakdown of NaCl is studied by Braunlich et al., [30], they found the dynamics of free carrier generation in NaCl and of laser energy transfer to the lattice greatly altered by the efficient and rapid formation of primary defects. Yet, the laser damage threshold at  $\lambda=532$  nm remains virtually unaffected by these photo-chemical processes. They identify two opposing causes for this outcome: removal of free carriers by photon absorption during formation and decomposition of these primary defects.

Casper et al. in 1990, [31] suggest that laser-induced stable F-centers play a significant role in multishot, bulk laser damage in KBr and KI at 532 nm. The production of stable F-centers is a result of laser induced electron-hole pair generation and is accompanied by an expansion of the crystal lattice. The nonuniform coloration produced by the focused laser beam leads to a buildup of local stresses resulting ultimately in catastrophic damage of the crystal.

The self-trapped-exciton recombination-luminescence technique is used to measure the three-photon-absorption cross section in KI at 532 nm by Kelly et al. in 1990, [32], and they measured  $\pi$  and  $\sigma$  luminescence provides a stringent test of the intrinsic single-shot damage process considered to be non-linear absorption of light by three-photon-generated free carriers.

Measurements were made of the absorption change at the F band and of the singlet luminescence in NaCl, induced by photoexcitation of the lowest state studied by Soda and Itoh [33]. They found, stability of the created F centers in NaCl is to be lower than in other alkali chlorides.

Shen et al., [34] exploit recombination luminescence of self-trapped excitons for the measurement of the four-photon absorption cross section in KBr at 532 nm and  $\sigma^{(4)} = (2 \pm 1) \times 10^{-112} \text{ cm}^8 \text{ sec}^3$ . Shen et al. in 1988, [35], also studied intrinsic single-pulse optical damage in KBr at 532 nm and the self-trapped exciton recombination



luminescence and the temperature dependence of the luminous efficiency is utilized to measure the lattice temperature rise resulting from the interaction of KBr with intense laser pulses at 532 nm.

Gorshkov et al. in 1985, [36] studied optical study of nonlinear absorption of ultra violet laser radiation by alkali halide crystal during the generation of non-equilibrium carriers and comparison of laser photoconductivity data with measurements of nonlinear absorption in the UV range.

The luminescence spectrum of SrTiO<sub>3</sub> from 1.6 to 3.2 eV has been studied by Leonelli and Brebner in 1986, [37] as a function of time elapsed after excitation. They associated the first one with self-trapped excitons interacting with acoustic phonons and the second with the retarded formation of self-trapped excitons from localized electrons and holes.

Epifanov et al.,[38] presented theory of avalanche ionization induced in transparent dielectric by an electromagnetic field and a diffusion approximation of the quantum kinetic equation for conduction band electrons obtained the region of its applicability investigated. Avalanche ionization produced in solids by large radiation quanta and relative role of multiphotonionization in laser induced breakdown which is studied by Gorshov[39]. State of the electron-avalanche theory and a comparison with experimental data are presented by Epifanov[40].

In 1989, Shen [41] reported free electron absorption of 1064 nm photons is measured photoacoustically in NaCl and SiO<sub>2</sub>. The electrons are generated with a 266 nm pump pulse by two-or-three-photon transitions.

# CHAPTER 3

## THEORY

### 3.1 THE PHYSICAL PROPERTIES OF CRYSTALS

#### 3.1.1 Alkali Halides (Ionic Crystals)

The alkali halides are typical ionic compound and their physical properties are in general well known. The most of the alkali halides crystallize in the rock salt structure, shown in Figure 3.1. In this structure each cation (alkali metal ion) is surrounded by (or "coordinated" with) six nearest- neighbor anions (halogen ions), and each anion by six nearest- neighbor cations. Ionic compounds (alkali halides) of the type  $M^+Y^-$  where  $M$ , group I alkali metal and  $Y$  group VII halogen. The cations and anions are each situated on the points of separate *face-centered* cubic lattices, and these two lattices are interleaved with each other.

The alkali halides are readily obtainable in a reasonable degree of chemical purity and can be grown in the form of single crystals with comparatively little difficulty.

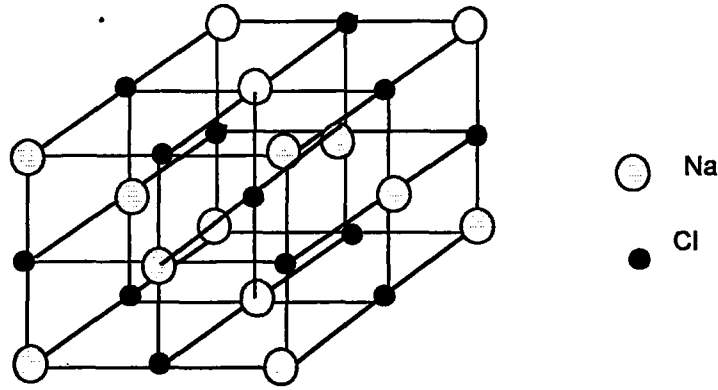


**Figure 3.1** The structure of the NaCl-type alkali halide

Stoichiometric ionic crystals are good insulators and conduction by electrons or holes is usually negligible. The band gap is so large that even at temperatures close to the melting point very few electrons are excited into the conduction band. For example, it is instructive to compare a typical ionic crystal such as NaCl (band gap  $E_g \cong 5$  eV) at 1000K with pure silicon (Si,  $E_g \cong 1.14$  eV) at 300K, which is itself quite a good insulator. Using the expression  $n \propto \exp(-E_g/2kT)$

$$\frac{n_{NaCl}}{n_{Si}} = \frac{\exp\left(-5 / (2 \times 8.6 \times 10^{-5} \times 1000)\right)}{\exp\left(-1.14 / (2 \times 8.6 \times 10^{-5} \times 300)\right)} \approx 10^{-3} \quad (3.1)$$

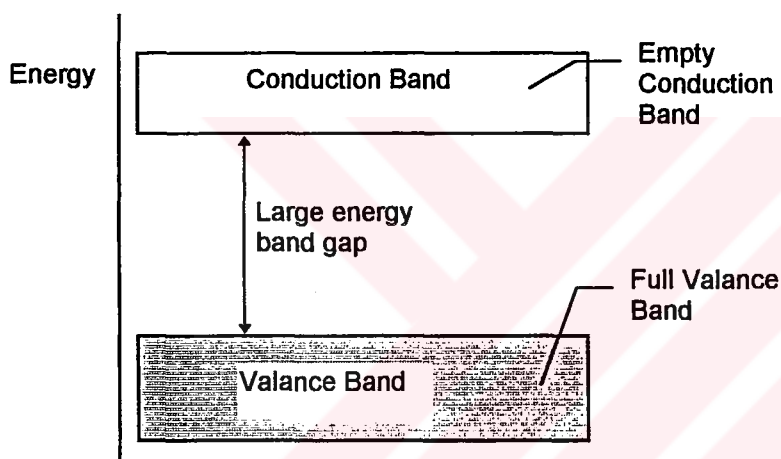
The conductivity of the ionic crystal even at 1000K would be  $10^{-3}$  times that pure Si at 300K, that is about  $10^{-6} (\Omega m)^{-1}$ . This still represents a very good insulator.

Nevertheless, ionic crystals do conduct electricity at high temperatures. The conductivity process does not, however, involve the motion of electrons, but instead

*charged ions* move through the crystal. Actual transport of matter (the ions) is therefore involved, this conductivity process is called ionic conductivity. That is, the carriers of electric charge are ionic, not electronic.

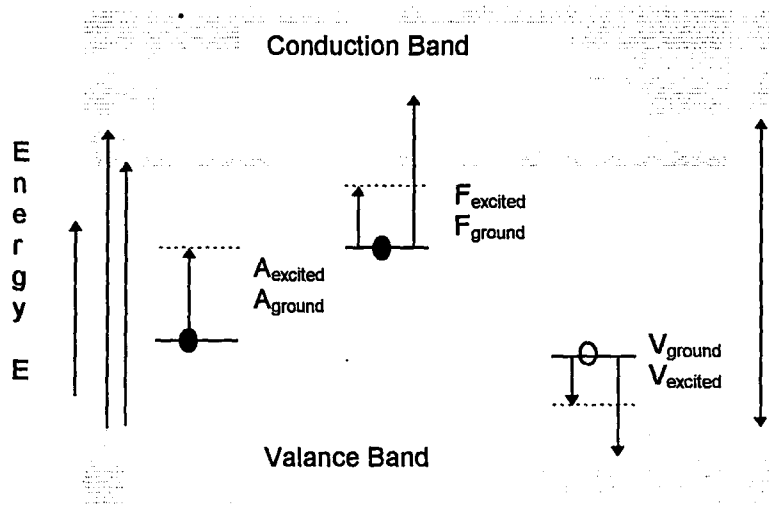
### 3.1.2 Energy Band

Figure 3.2 shows an energy diagram for an insulator. The main characteristic of an insulator, as can be seen in the diagram, is that the full valance band lies well below an empty conduction band. For a crystal without lattice defect there are no energy levels between the valance and conduction band. The energy levels introduced



**Figure 3.2** Energy band diagram for an insulator.

may be discrete or may be distributed depending upon the nature of the defect of the host lattice. These imperfections, impurities, intrinsic and extrinsic defects give rise to the localized energy level within the forbidden energy gap. Figure 3.3 shows band picture of an alkali halide, showing energy levels and some optical absorption due to imperfections.



**Figure 3.3** Energy band with some energy levels

Absorption of light in the far ultraviolet or irradiation with  $\alpha$ ,  $\beta$ , and  $\gamma$  or with laser corresponds to the liberation of an electron from the valance band into conduction band . When the valance band arises from the valance electrons of the halide ions, this corresponds to the removal of an electron from a halide ion. This deficiency of an electron is called a " positive hole", and the behaves like an electron with a positive charge.

Because a freed electron in the conduction band and the resulting positive hole in the valance band are both free to move, photoconductivity should results from this process, in principle. Absorption of light in the longest wavelength ultraviolet bands does not produce photoconductivity. Light of this wavelength is not sufficiently energetic to separate completely the electron and the positive hole, which remain bound to each other by Coulomb attraction. The electrically neutral entity thus formed is an excited state of

the crystal. The mobile "particle" consisting of an electron bound to a positive hole is called an "exciton".

### 3.1.3 Alkali Halide Imperfection

The crystalline solids are characterized by a regular and highly- ordered structure. The internal, long- range regularity of atomic packing is frequently reflected in the external form of synthetic and naturally occurring crystals. In these solids quite beautiful confirmation and extension of the evidence for crystallinity is obtained from X- ray diffraction studies. In terms of the ideal perfect crystal, atomic vibrations and excited electrons can be regarded as defects. Furthermore simple thermodynamic reasoning demonstrates that at equilibrium, there are present at any non- zero temperature both vacant lattice sites and interstitial atoms. Figure 3.4 shows the various point defects that can exist in a crystal. Important defects present in real solids are :

- Interstitial ions
- vacant lattice sites
- impurities
- dislocations.

At all temperatures above absolute zero, the atoms in a solid are subject to thermal vibrations. This means that they continuously vibrate about their equilibrium position in the lattice with an average amplitude of vibration that increases with increasing temperature. At a given temperature there is always a wide spectrum of vibration amplitudes, consequently occasionally in a localized region the vibrations may be so intense that an atom is displaced from its lattice site and a vacancy is formed. The displaced atom can either move into an interstice, in which case it is called a *self - interstitial*, or on to a surface lattice site. The vacancy self - interstitial is known as a Frenkel defect and the simple vacancy itself as a Schottky defect (Figure 3.5 ).

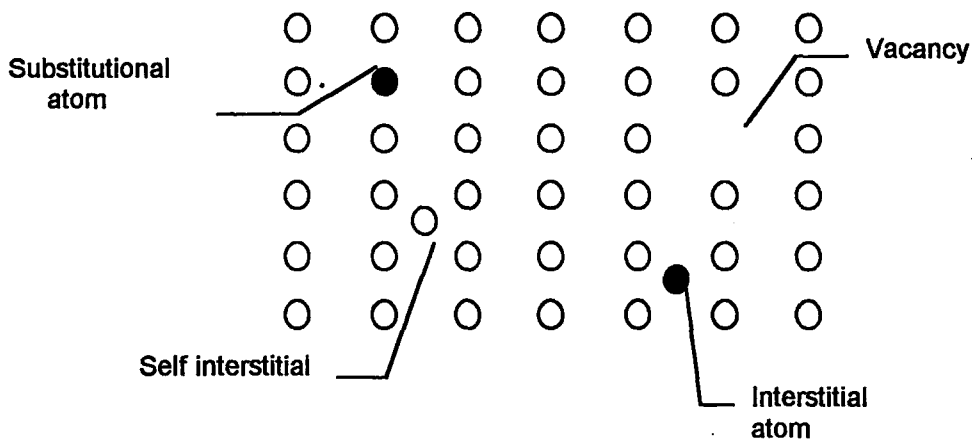


**Figure 3.4** The various point defects that can exist in a crystal.

### 3.1.4 Production of Color Centers

Color centers can be generated in a crystal by variety of techniques. The most of these are :

- Additive coloration,
- electrolytic coloration,
- exposure to ionizing radiation,
- laser damage.

Additive coloration; an excess of either alkali or halogen constituent can be introduced into an alkali halide crystal by heating the crystal to a high temperature in the vapor of the constituent. In electrolytic coloration; when a voltage is applied, a cloud of color enters from the pointed electrode and moves through crystal. Coloration by ionizing radiation includes all source that can generate free electrons and holes in the material. Since we will be interested in the laser damage techniques in this work .

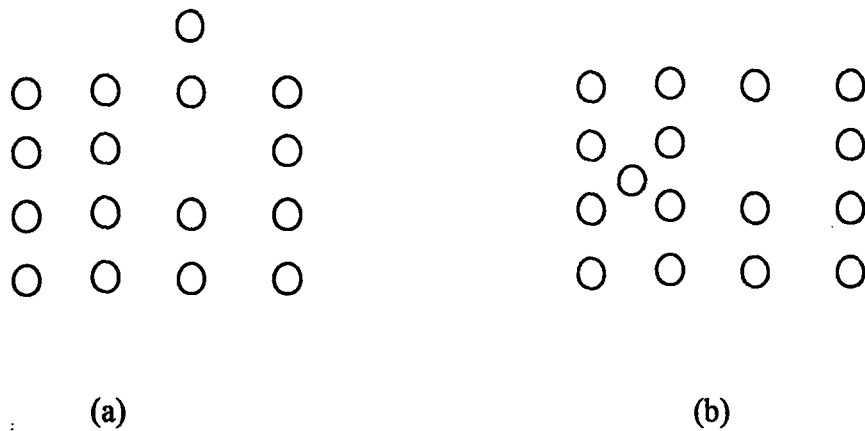


**Figure 3.5** The formation of a) a Schottky defect b) a Frenkel defect.

### 3.1.5 Definition of Laser Damage and Mechanism of Valance Electron Excitation

We briefly describe the phenomenon of laser damage of transparent materials and two mechanism of valance electron excitation invoked to explain it.

#### a) Laser Damage

Intrinsic laser damage of transparent solids is the irreversible modification of a nominally pure material as a result of exposure to a laser beam (pulse or continuous wave) of sufficiently high intensity. (Extrinsic laser damage is defined as that arising from, for example, metal particles or other absorbing inclusions). Such damage is believed to be threshold phenomenon, i.e., laser pulses of peak intensity below the breakdown threshold,  $I_B$ , do not cause damage while those above do. Experimentally, damage is defined by optically observable with (naked eye or a microscope) breakdown of the crystal structure[3]. As such, it represents a light scattering center and can therefore also be observed by visible laser light scattering. In experiments measuring bulk damage threshold (as opposed to surface damage), a laser pulse is tightly focused in the bulk and damage occurs in a region surrounding the focal point. This damage is believed to arise



by valance electron excitation and their subsequent transfer of light energy to the crystal lattice via Joule heating and subsequently melting the solid in the interaction region. For theoretical purposes, damage either arises when the melting temperatures is reached (in calculations) or a critical density of conduction electrons (usually taken as  $10^{18} \text{ cm}^{-3}$ ) is excited to create an opaque absorbing plasma. The damage threshold depends on wavelength and laser pulse length, and theoretical models rely on this dependence for experimental verification. The experimental definition given above is not the only possible on, and it has been suggested that it needs to be modified due to observed irreversible changes in the bulk absorption following pulses that did not create damage according to the traditional criteria[42].

### **b)Electron Impact Ionization**

Laser damage is widely regarded to be a result of avalanche formation by electron impact ionization when multiphoton generation of free carriers is inefficient. The major point of argument is under what conditions do these competing mechanisms dominate the process.

Avalanche formation is described as follows: a low concentration of conduction electrons (generally assumed to be  $\approx 10^{10} - 10^{13} \text{ cm}^{-3}$ ) generated during the early part of a laser pulse from shallow traps or defect state by single -or low-order multiphoton absorption, absorbs additional energy from the laser photon field while simultaneously losing energy to the lattice through electron- phonon collisions. If the average rate of energy gain (dependent on the field strength) is greater than the energy loss rate, then a fraction of the electrons will obtain sufficient kinetic energy ( $E_{\text{gap}}$ ) to excite valance electrons to the conduction band by impact ionization. This process continues, and as the electric field in the pulse increases towards the peak value, impact ionization generates an electron avalanche in the conduction band, described by the equation  $\frac{dn_c}{dt} = \gamma(E)n_c$ , where  $n_c$  is the free carrier density and  $\gamma(E)$  is the avalanche rate ( $\text{sec}^{-1}$ ) as a function of

the electric field E. The energy these carriers lose in electron- phonon collisions eventually results in the lattice melting for pulses above the breakdown intensity threshold. The precise nature of conduction electron energy loss and gain apparently depends on the laser frequency and the electron- phonon collision frequency.

### c) Multiphoton Absorption

When the photon energy becomes a significant fraction of the band gap of the transparent material, generation of free carriers by multiphoton absorption of valance electrons supplements or replaces impact ionization in the damage process. An extensive review of theoretical and experimental results pertaining to multiphoton absorption in crystalline solids was recently performed by Nathan et al. [43].

The mathematical expression for the transition rate in an m-photon absorption process obtained from m<sup>th</sup> order time-dependent perturbation theory can be reduced to the simple form

$$\Gamma_m = \alpha^{(m)} I_m \quad (3.2)$$

where  $\Gamma_m$  is the m<sup>th</sup> order transition rate (sec<sup>-1</sup>), I is the light intensity and  $\alpha^{(m)}$  represents the m-fold summation of the interaction matrix elements over the unperturbed eigen states. The free carrier generation rate can be written as

$$\frac{dn_c}{dt} = N\sigma^{(m)} F^m \quad (3.3)$$

where  $\sigma^{(m)}$  is the generalized m-photon absorption cross section in units of ( $\text{cm}^{2m} \text{sec}^{m-1}$ ),  $F = \frac{I}{\hbar\omega}$  is the photon flux in units of (photons/cm<sup>2</sup>.sec), and N is the density of absorbing species. In our case N represents the density of Cl<sup>-</sup> ions (in cm<sup>3</sup>) in the crystal, since for polar crystals the highest valence electrons are localized on the anions and each Cl<sup>-</sup> can lose only one electron before binding with a neighboring Cl<sup>-</sup> to form a Cl<sub>2</sub><sup>-</sup> molecular ion.

The theoretical and experimental values of  $\sigma^{(m)}$  is difficult to obtain with increasing order m, such that two-photon absorption has been quite absolutely investigated and three-photon absorption less so, while results for fourth and higher order multiphoton absorption are very sparse. Most of the data that do exist for high order nonlinear absorption were obtained in alkali halides.

## 3.2 Color Centers

The possibility of absorbing light of energy less than the band gap energy makes the crystal colored and the imperfections which give rise to these absorption are called "*color center*". These are trapped electron centers in crystal, trapped electron centers with foreign ions trapped hole centers, and chemical defect.

### 3.2.1 Electron Centers

#### F-Center

The F-center is a prototype for all defect studies, the F-center, an electron trapped at an anion vacancy is the best-understood point defect in ionic crystals as seen in Figure 3.6. F-centers have a wide electronic absorption band in the visual range of the spectrum. The presence of the F-centers in a crystal thus results in a coloration of the

alkali halide, which is normally transparent for visible light. The F-center is one of the simplest examples of a system with a strong electron- phonon coupling.

In most host lattice the absorption of light by the F-center is followed by emission of light with a longer wavelength. This so- called Stokes shift occurs because the F-center releases a large part of the energy it absorbed to the vibrations of the lattice, i.e. this energy is converted into heat. The normal optical cycle is as follows: After the optical absorption, the center undergoes lattice relaxation until it reaches the so- called relaxed excited state (RES). From the relaxed excited state a radiative electronic relaxation process occurs on the time scale of about a microsecond. The cycle is closed by further lattice relaxation.

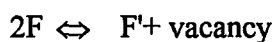
Exceptions to this rule are NaBr, NaI and the Lithium halides. In these crystals the F-center luminescence is (almost) completely quenched by a radiationless electronic relaxation process. This nonradiative relaxation may occur in two ways, namely either during the lattice relaxation which brings the F center to the relaxed excited state, or after the lattice relaxation.

In the first case, the nonradiative transition has to compete with the lattice relaxation to the relaxed excited state, which means that it must be highly efficient. The lattice relaxation will determine the time scale of the electronic relaxation, which must then be between 100 femto second to 10 pico second ( $1 \text{ Psec} = 10^{-12}$ , 1 femto second is 1/1000 of a pico second). In the second case, the nonradiative transition has only to compete with the (micro second) radiative transition from the relaxed excited state, which means that it can be much slower.

F-center is a simple intrinsic defect, and since the position of the absorption band is independent of the alkali metal used to color the crystal by non-Stoichiometry, the two obvious models are a halogen vacancy or a metal interstitial. The vacancy site would trap an electron, since this maintains the charge neutrality of the perfect lattice.

## **F'- CENTER**

F'-center consist of an F-center plus a second weakly bound electron as seen in Figure 3.6. The small attractive potential for this electron means that the wave- functions extend over several atomic neighbors away from the center. By comparison with the F-center this produces a broader, lower energy absorption band whose width is insensitive to the temperature changes, since many atoms are involved and the atomic energy levels are shallow. The center is thermally and optically unstable and is in equilibrium with the F-centers by a reaction



At high temperatures the F'- center decays and reforms F-center.

### **Trapped Electron Centers With Foreign Ions**

When an alkali halide doped with a monovalent or divalent foreign alkali ions is irradiated, the electrons and holes can be trapped by the dopants, or by the defects produced by the irradiation, or by dopant- vacancy complexes. Especially informative and easy to produce are foreign ion defect. Much attention has been given to foreign cations. In the case of  $F_A$  centers (see in Figure 3.6 ) these are monovalent foreign alkali ions ( $Na^+$  in KCl) in the case of  $F_Z$  centers they are divalent ions ( $Ca^{++}$  in KCl) which are nearest neighbor to the anion vacancy.

#### **3.2.2 Hole- Trapping Centers**

Trapped electron centers such as F, F aggregate,  $F_A$ ,  $F_Z$ , centers are lattice- defect centers. Their properties like structure, energy levels, phonon- electron coupling and electron wave distribution are primarily given by the lattice and lattice defects (vacancies). Trapped hole centers (V centers) are characterized primarily by molecular

properties. They are molecules or molecular ions imbedded in lattice defects, with very loose lattice interaction only. Electronic centers may be considered as alkali excess centers if we consider only the deviation from stoichiometric equilibrium. Hole centers however may indeed be considered as halogen excess centers.

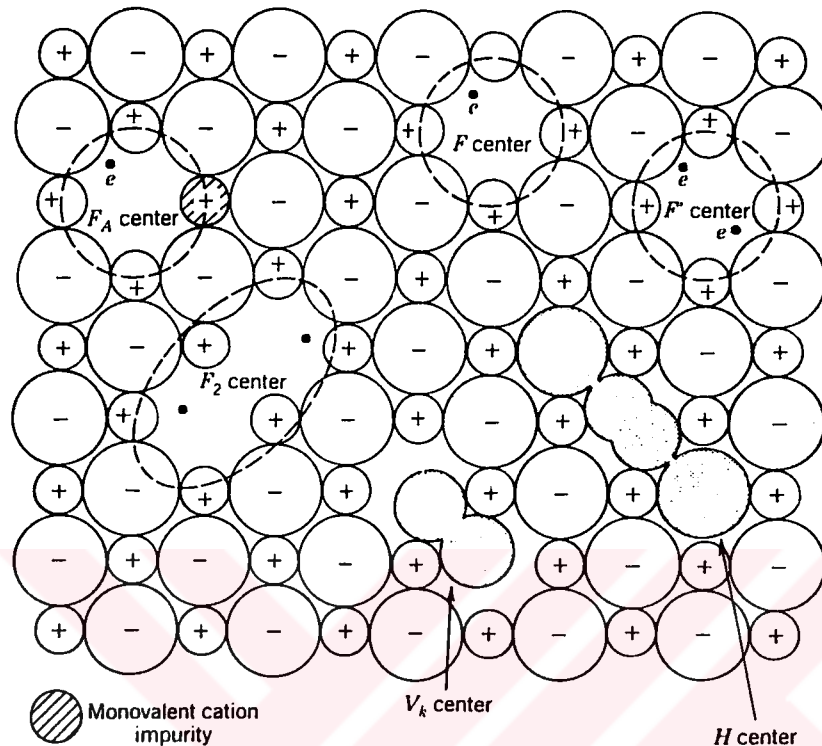


**Figure 3.6** Common color centers in alkali halides  $MX$ . These include electron- excess enters, notably the F center and related defects (the F' center has an extra electron; the  $F_A$  center is an F center with an adjacent cation impurity; the  $F_2$  center is two adjacent F centers), and two centers involving  $X_2^-$  molecular ions, namely, the self-trapped hole ( $V_K$  center) and neutral anion interstitial(H center).

Trapped hole centers are produced by similar techniques to trapped electron centers. If an alkali halide is radiated with X,  $\alpha$ ,  $\gamma$ ,  $\beta$  ray or laser pulses at room temperature or if it is irradiated at low temperature and warmed to room temperature, the  $V_2$  and  $V_3$  bands are observed. If the crystal is irradiated at  $-180^\circ\text{C}$  and measured at this temperature without warming up the  $V_1$  band is observed. The models of the V centers are shown in Figure 3.7. The H center is known to be a hole trapped at an interstitial halide ion and it has  $\langle 110 \rangle$  symmetry as  $V_K$  center.

## The $V_K$ Center

Two lattice anions with filled electronics shells are combined by the trapping of one hole forming a molecular ion of the type  $F_2^-, Cl_2^-, Br_2^-$  with reduced interatomic distance see Figure 3.8. These molecules are orientated along one of the six  $\langle 110 \rangle$  directions.

The  $V_K$  center is a good example of a molecule-in-a-crystal defect, that is, the host weakly perturbs the  $X_2^-$  molecular ion.

$V_K$  centers decay after trapping electrons which are released by ionization of electron centers. The molecular ions split into two normal lattice ions:



The internuclear distance of the  $X_2^-$  molecule ion is intermediate between the separation of the halide ions in the unperturbed crystal and the separation in the neutral halogen molecule. Thus the  $V_K$  center is formed by the loss of an electron from a halide ion, followed by the pulling together of the resulting atom with an adjacent normal halide ion (see in Figure 3.6).

## The Self-Trapped Exciton (STE)

The self-trapped exciton in alkali halide is essentially a self-trapped hole to which an electron is bound, that is  $[V_K e]$  or  $[he]$ . There are at least three types of excited state of the self-trapped exciton: electron-excited states  $[h e^*]$ , hole-excited states  $[h^* e]$ , and states with both components excited  $[h^* e^*]$ . These excitations are distinct in energy and readily characterized. Nonradiative transitions can take the center from one type of state into another. The hole excitations are only weakly perturbed from those of the  $V_K$  center

into another. The hole excitations are only weakly perturbed from those of the  $V_K$  center by the presence of the electron. The electron excitations, with the electron moving in the field of a localized positive charge, resemble those of a hydrogen atom, apart from the axial perturbation that splits  $p$  states into axial  $\sigma$  and equatorial  $\pi$  states. The singlet and triplet excitons can occur, depending on whether the electron and hole antiparallel or parallel spins. The triplet form can only recombine by a spin-forbidden transition. The lowest triplet state has a long lifetime, of order  $10^{-3}$  sec, and a whole range of spectroscopic measurements can be made on it, including optical absorption, luminescence.

The self-trapped excitons shows enormous variety to the various transitions observed. The two principal luminescence transitions give the so-called  $\pi$  and  $\sigma$  bands with dipoles respectively normal and parallel to the axis of the self-trapped hole. The long-lifetime  $\pi$  band is seen in all alkali halides, its produced by decay of the lowest triplet state to the crystal ground state (electron-hole recombination); in the triplet, the hole is in essentially a  $V_K$  center ground state. The rapid  $\sigma$  transition is seen some alkali halides.

### 3.3 THE CHARACTERISTIC OF THE F-BAND ABSORPTION

The F- band absorption is a simple bell-shaped absorption band whose spectral position and width depend on the nature of the alkali halide and on the temperature. For alkali halides having the NaCl structure, it was found empirically by Mollwo-Ivey was derived a more accurate empirical relation

$$\lambda_{\max} (\text{in } \text{Å}) = 703 d^{1.84} \quad (3.5)$$

where  $\lambda_{\max}$  is maximum wavelength,  $d$  is the lattice constant of the alkali halide in Angstrom units. Table 1 lists the wavelengths of the peak of the various of the defect centers in several alkali halides.



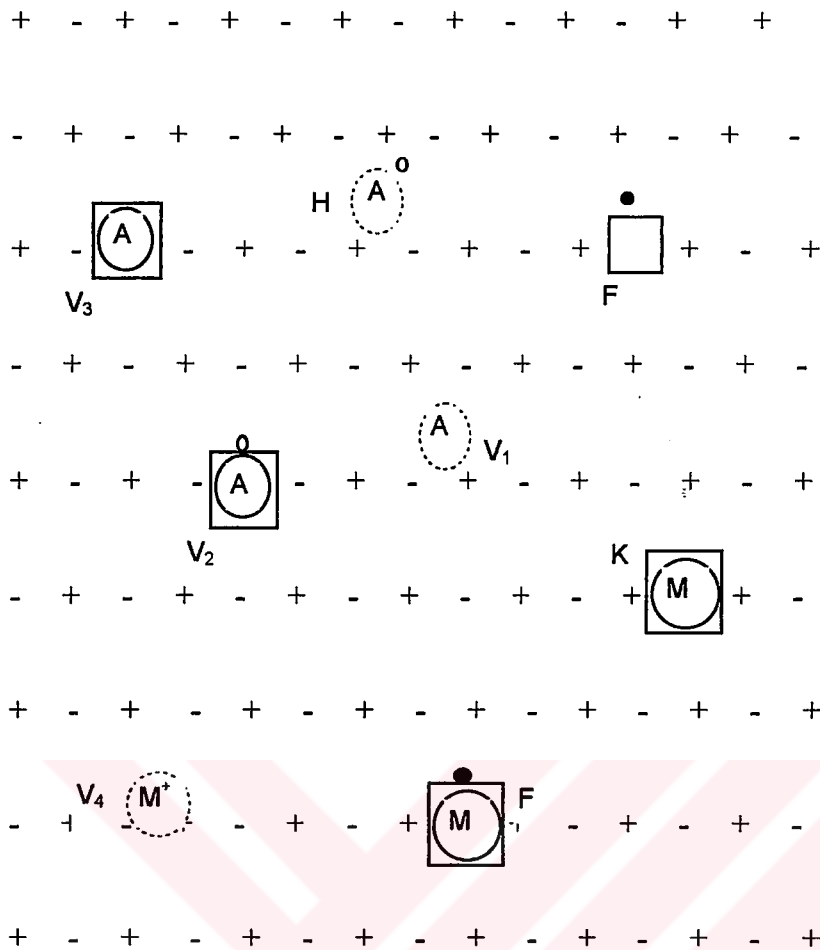


**Figure 3.7** Models of color centers from Schulman and Compton. The H, V<sub>1</sub> and centers have tetrahedral symmetry; the V<sub>2</sub>, V<sub>3</sub> and other centers have cubic symmetry.

- |                   |                                  |     |                      |
|-------------------|----------------------------------|-----|----------------------|
| ●                 | Trapped electron                 | (M) | Metal atom           |
| □                 | Positive or negative ion vacancy | ○   | Positive hole        |
| (A)               | Halogen atom                     | (A) | Interstitial halogen |
| (M <sup>+</sup> ) | Interstitial metal ion           |     |                      |

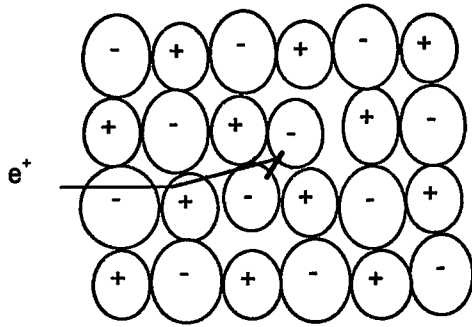


**Figure 3.8** Atomic structure of the  $V_K$  center

F-band in a typical alkali halide depends on the temperature with decreasing temperature the band becomes narrower and its peak position shift to shorter wavelengths. At higher temperature, but at low width varies as  $T^{1/2}$ , where  $T$  is the absolute temperature, but at low temperature the width approaches a limiting value of a few tenths of an electron volt. It is described by

$$W = A [\cot (h\nu_g/2kT)]^{1/2} \quad (3.6)$$

where  $A$  and  $\nu_g$  are constants,  $h$  and  $k$  are Planck's and Boltzmann's constants respectively,  $W$  is the "half width" or width at half-maximum of the F- band.  $W$  is the separation in energy units between the two points on the absorption curve where the absorption constant is one-half of its value at the peak of the curve.

Comparison of the frequencies  $w$  with the theoretical phonon spectrum suggests that the phonons responsible for the F-band width lie in the acoustic branch for alkali halides with light atomic masses (LiF, NaF, NaCl) and the optical branch for those with longer atomic masses (KI, KBr). This is a rather broad generalization, however, since the acoustic and optic phonon branches usually overlap.

If assuming that the centers giving rise to the absorption do not interact with one another, the area under the absorption curve directly proportional to the concentration of the absorbing centers. The simple bell-shaped of the F-band suggests that the absorbing centers can be treated as damped oscillators according to classical dispersion theory. This was first done by Smakula.

$$Nf = \frac{9mc}{2e^2} \frac{n}{(n^2 + 2)^2} \alpha_{\max} W \quad (\text{for a Lorentizan band}) \quad (3.7)$$

$$Nf = 0.87 * 10^{17} \frac{n}{(n^2 + 2)^2} \alpha_{\max} W \quad (\text{for a Gaussian band})$$

where,  $\alpha_{\max}$  is absorption coefficient in  $\text{cm}^{-1}$  at the peak of the absorption band, and  $W$ , the half-width of the absorption band in electron volts,  $N$  is the number of F center per  $\text{cm}^3$ ,  $f$  is "oscillator strength",  $n$  is the refractive index of the crystal for wavelength at the peak of the absorption band,  $m$  is electron mass,  $c$  is the velocity of light,  $e$  is the electron charge.

### 3.4 CONFIGURATION CO-ORDINATE DIAGRAMS

The optical properties of solids are determined by the way in which the electrons in the material can respond to radiation. Optical techniques have been applied extremely successfully to the study of defects in ionic crystal, and to a lesser extent in semiconductors. Free electrons in metals cause almost total reflection of photons of all energies, and hence studies are restricted to reflectivity measurements. Optical absorption at a lattice defect are determined by the ground and excited energy states of the center. This results in an absorption spectrum with lines at a certain energy and a certain line shape. It is clear that the most obvious difference between various types of defects is the

energy of a specific absorption line. When the center is excited by the absorption of a photon, the average electronic distribution is changed and after sufficient time the ions move to new equilibrium position.

The shape of optical absorption curve is described by a configuration co-ordinate diagram as shown in Figure(3.9).

**TABLE 1** Wavelengths of the absorption peaks arising from various trapped-electron and trapped-hole centers in the alkali halides [21].

Center	F	F'	F'	H	V <sub>1</sub>	V <sub>K</sub>	V <sub>2</sub>	V <sub>3</sub>	V <sub>4</sub>
Temperature of observation (°K)	300	140	170	4	77	77	300	300	90
LiF	250					348			
LiCl	385								
NaF	341								
NaCl	458	510		330	345		223	210	
NaBr	540								
NaI	588								
KF	455								
KCl	556		750	335	356	365	230	212	~254
KBr	625		700	380	410	385	265	231	275
KI	689					404			
RbBr	694								
RbI	756								
CsCl	605								
CsBr	680								

Consider, the course of events during optical absorption or emission by the center. According to the Franck-Condon principle an electronic transition occurs in a short time interval, the ions are unable to move, i.e., the transition occurs with no change in the configuration coordinate of the ions. In Figure 3.9 absorption will occur at point A, the ground state equilibrium position, and point B the point on the excited state curve with the same configuration coordinate  $X_A$ , a photon must have the energy  $(E_B - E_A)$  to produce this excitation. B is in a state of excitation with energy  $(E_B - E_C)$  in excess of the equilibrium energy  $E_C$ . The nuclei move to their new equilibrium coordinate  $X_C$  with the loss of an amount of energy  $(E_B - E_C)$ . This energy appears as heat, i.e., as lattice vibrations. From point C the system can jump to D with the emission of a photon of energy  $(E_C - E_D)$ . This jump occurs with a probability per unit time of  $1/\tau$  (sec), where  $\tau$  is the radiative lifetime of the excited state. For an atomic center having an allowed transition which gives visible emission,  $\tau \approx 10^{-8}$  sec and is independent of temperature. The center then loses an amount of energy  $(E_D - E_A)$  in the form of heat as it relaxes from D to A. Since energy is lost as heat, it is obvious that  $(E_B - E_A)$  is greater than  $(E_C - E_D)$  (Stokes shift).

The system in the ground state will have  $\hbar\omega_g/2$  zero point energy and a distribution in coordinates that is Gaussian about  $X_A$ .  $\omega_g$  is a frequency characteristic of the breathing mode in the ground state. If the excited state curve at B is approximated by a straight line, this model predicts that the absorption curve will have a Gaussian distributed in energy.

The temperature dependence of the half-width of the absorption band can be predicted by considering the change in the distribution of the system about the point  $X_A$  with a change in temperature. The half-width  $W_{1/2}$  should be proportional to  $[\cot \hbar\omega_g / 2kT]^{1/2}$ .  $W_{1/2}$  is predicted to be constant for low temperatures and to vary as

$T^{1/2}$  at high temperatures. The half-width of the emission curve should be proportional to  $[\cot \hbar \omega_e / 2kT]^{1/2}$ .

Increase of temperature provides the activation energy  $U[(E_F - E_C)]$  required for a radiationless transition of the system from the excited state to the ground state of  $X_F$ . The efficiency of luminescence will be decreased by this. This is called "thermal quenching" of luminescence.

### **3.5 ELECTRICAL PROPERTIES OF CRYSTALS CONTAINING DEFECTS**

The uncolored alkali halides are insulating solids at normal temperatures and that they show electrolytic conductivity at high temperatures. Even when these crystals are additively colored to form the F- band, they remain insulators at normal temperatures in the dark. If they heated, electronic conductivity can be observed in addition to electrolytic conductivity. Photoconductivity is exhibited even at low temperatures when colored alkali halides are illuminated with absorbed in the F-band.

#### **3.5.1 Photoconductivity**

The light absorbed by the F-center can excite it to a bound electronic state, from which it can return to the ground electronic state either by luminescence or by a radiationless process. Thus, the main bell-shaped absorption band is presumably due to the transition of the F-center from the ground state to the first excited state. Although this absorption presumably does not correspond to direct ionization of the F-center, photoconductivity is nevertheless observed when the crystal is illuminated in this band. The photoconductivity of F-centered alkali halides is exceptionally simple. The photoconductivity produced by equal numbers of incident light quanta of different wavelengths in the F-band region is proportional to the absorption coefficient of the crystal for each wavelength. This implies that the quantum yield of free electrons is independent of the wavelength of the light absorbed in the F- band.

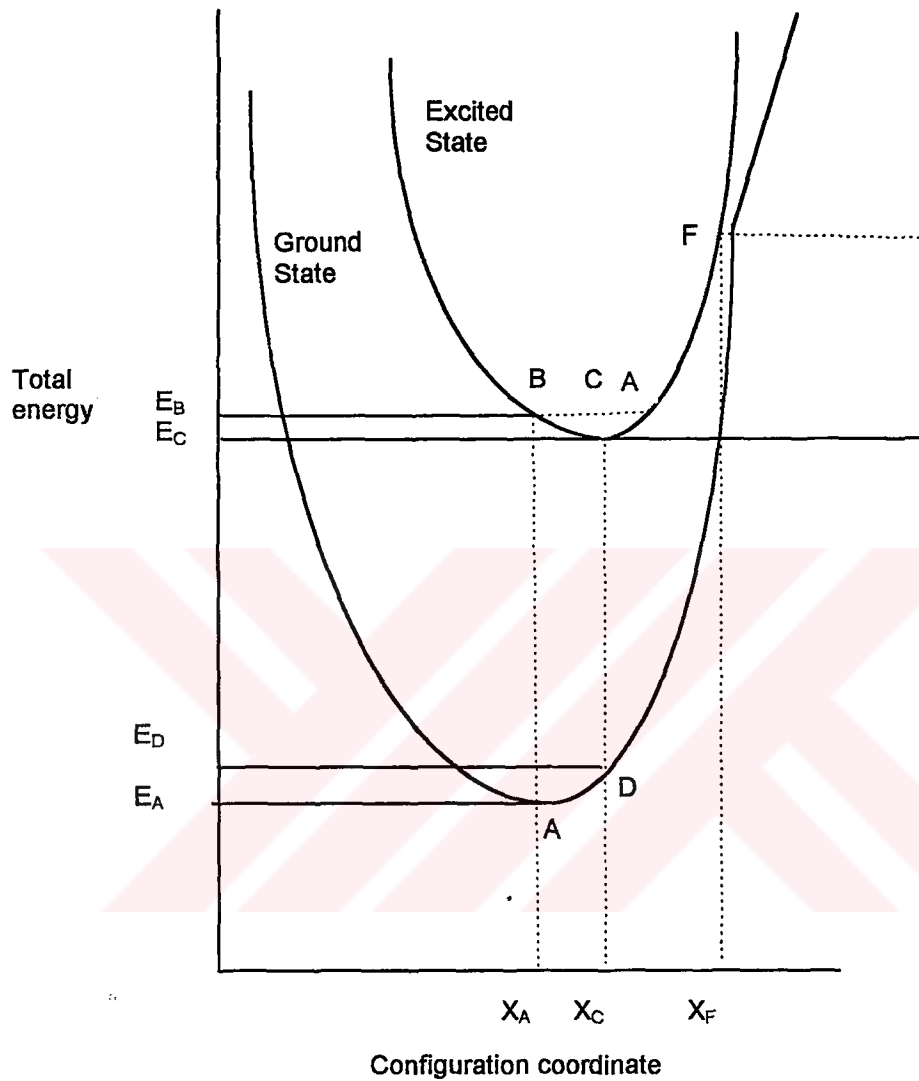


**Figure 3.9** Configuration coordinate diagram ( $A \rightarrow B$ ) absorption, ( $C \rightarrow D$ ) emission for a defect center.

Absorption of light does not eject the F-center electron into the conduction band directly, but raises it to a bound excited state. The excited F-center electron becomes a free charge-carrier because the thermal agitation of the lattice ejects the electron into the conduction band before it can drop back to its ground state in the F-center. The temperature dependence of the photoconductivity arises from the increased probability of ejecting an electron as the temperature increases.





# CHAPTER 4

## MICROSCOPIC PROCESS OF CRYSTAL-PHOTON INTERACTION

### 4.1 INTRODUCTION

As we have stated before, the total interaction between the laser photons and crystals is not only multiphoton electron-hole (e-h) pair generation but also the conduction band electrons can absorb energy from the photon field. They can so-called primary defects which are created as a result of e-h pair generation. The calculation of prebreakdown energy deposition in NaCl at 532 nm, four-photon excitation of valance electrons to the conduction band is needed, this is a primary absorption process. For this reason the four-photon absorption cross sections obtained from the data are overestimated. And unfortunately, the parameters needed to more completely model the overall interaction are not known to a high degree of accuracy.

There are two theories of lattice heating resulting from the absorption of photons by electrons in the conduction band. The first is the *Polaron model* proposed by Schmid et al. [5] in which the electrons are strongly coupled to the phonon system and absorption

of a single photon by an electron is followed by virtually instantaneous dissipation of the excess energy to the crystal lattice. The second one is *avalanche theory of free electron generation*. In both models phonons play the important role of the third particle for the electron to absorb electromagnetic energy, since a free electron cannot absorb single photons (energy and momentum cannot be conserved simultaneously in the two-particle electron-photon interaction). A polaron is the quasi-particle constructed from a propagating electron and the lattice distortion ("phonon cloud") which accompanies it. However, it is not clear whether a polaron which absorbs a photon of relatively high energy (e.g. 2.33 eV) remains a polaron since the coupling of electrons to longitudinal optical (LO) phonons is weaker when the electron energy,  $E$ , is above the bottom of the conduction band ( $E \gg \hbar\omega_{LO}$ ). That is, once the polaron absorbs a "large" photon, it may in fact become a "free" electron in the sense that free carrier heating of the type used in the avalanche theory may be more appropriate.

In addition to lattice heating by electrons in CB, the altered states of the lattice constituents following excitation of valence electrons results in hole ( $V_K$ ) centers which serve as electron traps. An electron trapped by a  $V_K$ -center can exist in hydrogen-like excited states before recombination (but direct recombination is also possible). The bound states of a  $V_K$  center plus electron are collectively known as a self-trapped exciton (STE). The  $V_K$  center and STEs are intrinsic to alkali halide crystals; i.e., no impurity is required for their formation, only excitation of valence electrons across the gap is necessary. An isomer of the lowest excited STE state, the close F-H pair, is also a possible result of the creation of e-h pairs. All of these intrinsic or primary crystal defects in alkali halides have been studied for many years and Braunlich et al. [30] were the first to introduce them to the field of laser damage as a mechanism for energy absorption. The STE, F-, and  $V_K$ -center all absorb 532 nm photons. We do not attempt to model effects due to impurities since their concentrations and absorption properties are not well known.

Also highly accurate absorption parameters for conduction electrons (free electrons or polarons), STE's and  $V_K$ -centers are not available, so that modeling of the

complex laser-crystal interaction parameters (e.g. absorption cross sections) relies on the best estimates we could obtain from literature. Jones[9] showed that the essential demonstration of the primary event of four-photon absorption, i.e., a nonlinear index of  $\cong 4$  for absorbed energy versus incident pulse energy. Their experiment was performed on a 4mm thick wafer cut from the middle of the first boule. This sample was chosen purposely to see if a wafer from the middle of the boule was clean enough to yield prebreakdown data. That the crystal quality is indicated by their observation that a sample from near the bottom of the boule did not yield a signal attributable to four-photon absorption before damage. The data for this calibration are the lower set of eight in Figure 4.1. The upper limit of the four-photon absorption cross section obtained from the data set is  $\sigma^{(4)} = (5.7 \pm 2.5) \times 10^{-113} \text{ cm}^8 \text{ sec}^3$  and the data of the second wafer from the top of the first boule are higher set of points in Figure 4.1. They presented two different samples from the same boule in same graph with slope of line in the double-logarithmic plot is  $(3.8 \pm 0.14)$ .

## **4.2 ELECTRON-HOLE PAIR GENERATION, PRIMARY DEFECT PRODUCTION AND SECONDARY ENERGY ABSORPTION**

### **4.2.1 Four Photon Electron-Hole(e-h) Pair Generation**

In general, the avalanche mechanism results in a free carrier generation rate of

$$dn_c/dt = N\sigma^{(4)}F^4, \quad (4.1)$$

where  $n_c$  is the conduction electron density,  $N$  the density of active atoms, and  $F$  the laser photon flux.

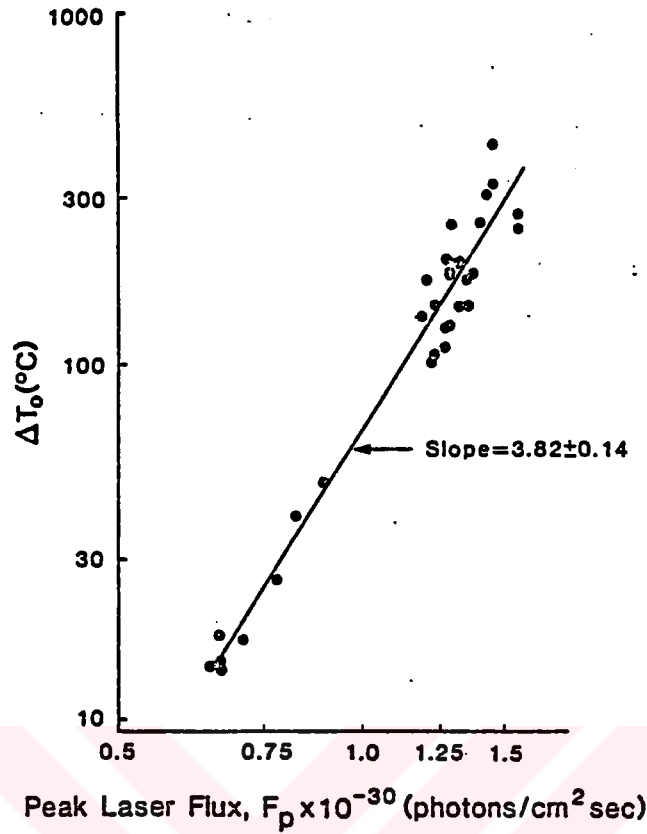


**Figure 4.1** Composite double-logarithmic plot of temperature increase at focal point vs incident energy of 532nm pulses

#### 4.2.2 Avalanche Generation and Free Carrier Heating

The avalanche mechanism results in a free carrier generation rate of

$$\frac{dn_c}{dt} = \gamma n_c \quad (4.2)$$

where  $\gamma$  is the avalanche coefficient, a very complicated function of crystal properties, photon energy and electric field strength. Electrons in the conduction band (the bottom of which we assign the zero of energy) gain and dissipate energy via electron-photon-phonon interactions. If some of them gain more kinetic energy than they lose, then impact

ionization of valance electrons can occur when a conduction electron obtains kinetic energy equal to the band gap of the crystal, resulting in electrons of approximately zero energy which can then both be accelerated and ionize further valance electrons and so on. If the avalanche multiplication parameter  $\gamma$  is sufficiently large, this impact ionization creates an enormous number of conduction electrons very rapidly and their interaction with phonons leads to significant heating of the lattice. The form of the avalanche rate function  $\gamma$  depends to a large extent on the relation of the photon energy,  $\hbar\omega$ , to the band gap energy  $E_g$ .

For 532 nm photons interacting with conduction electrons in NaCl ( $E_g = 8.6$  eV), the avalanche coefficient  $\gamma$  is given by Gorshov et al.[39]  $\gamma = Q(1) \gamma_0$  where for a four-photon band gap  $\gamma_0 \approx (4^6/4!)(q\delta)^5$ ,  $Q(1)$  is the constant at which electrons lose energy by acoustical phonon scattering ( $Q(1) = 5 \times 10^{13} \text{ sec}^{-1}$  which is approximately the one-tenth electron-phonon collision frequency, which is estimated to be  $\approx 6 \times 10^{14} \text{ sec}^{-1}$  in Ref. 29 and 43)  $q\delta$  is a dimensionless product,  $q\delta \cong a (T/T_0) E^2$ , which arises from the solution of the diffusion equation, where  $E$  is the electric field maximum amplitude,  $T$  is the lattice temperature,  $T_0 = 300$  K, and  $a$  is coefficient with  $e^2 k T_0 / 6 m^2 v_s^2 \omega^2 E_g \cong 5 \times 10^{-16} (\text{cm/V})^2$  where  $e$  and  $m$  are the charge and mass of electron,  $k$  is Boltzmann's constant, and  $v_s$  is the longitudinal sound velocity. When  $E$  is expressed in V/cm,  $a$  lies in the range  $3 \times 10^{-17} (\text{cm/V})^2 \leq a \leq 1 \times 10^{-15} (\text{cm/V})^2$ .  $E^2$  (in  $(\text{V/cm})^2$ ) =  $240\pi I/n(\text{W/cm}^2)$ , where  $n$  is the index of refraction.  $F = I/\hbar\omega$ ,  $E^2 = 240\pi \hbar\omega F/n$ . We get  $\gamma$ ,

$$\gamma = 5 \times 10^{13} \gamma_0 \text{ sec}^{-1} \approx 1.5 \times 10^{-62} [a(T/T_0) F/n]^5 (\text{sec}^{-1}), \quad (4.3)$$

with the magnitude of  $a$  being between  $3 \times 10^{-17} \leq a \leq 1 \times 10^{-15}$  this uncertainty arising from uncertainties in the effective mass of electron and collision frequencies. This uncertainty in  $a$  leads to an enormous uncertainty in  $\gamma$ , which demonstrates the difficulties encountered in modeling the interaction of laser photons with wide gap materials. Jones et al.[9] have named  $a$  the "the rubber parameter" due to its extreme flexibility.

The lattice heating due to the electron- phonon scattering implicit in the avalanche generation of free carriers can be reduced to

$$\rho c(dT/dt) \approx (mkT/2\pi)^{1/2} (eE/m\omega)^3 (n_c/l_{ac}v_s) \quad (4.4)$$

where  $l_{ac}$  is the mean free path of an electron between collisions with acoustic phonons. Also uncertainty arising from effective mass of the carriers,  $m$ , the mean free path  $l_{ac}$ . Since both of these parameters are functions of the electron energy, assuming some sort of intermediate values. The effective mass of a low energy carrier may be as low as  $0.5 m_e$  ( $m_e$  = free electron mass), assuming  $m = 0.75 m_e$ . The electron mean free path is estimated by  $l_{ac} \approx v \tau_{coll}$ , where  $v$  is the electron velocity and  $\tau_{coll}$  is the reciprocal collision frequency. The average energy of the free carriers under pre-damage conditions is probably considerably less than  $E_g/2$  ( $\approx 4.3$  eV for NaCl) and so  $l_{ac} \approx 10^{-7}$  cm, lattice heating relation is obtained by Jones[9] with these results,

$$\rho c(dT/dt) \approx 8.3 \times 10^{-29} E^3 T^{1/2} n_c \text{ (Joules/cm}^3\text{sec)}, \quad (4.5)$$

where  $E$  is the electric field strength (V/cm). This value is highly uncertain which is the typical case in the avalanche-related calculations.

Avalanche-only carrier generation mechanism, is used to computation of heating, a number of electrons must be initially present in the conduction band, supposedly arising from shallow electron traps imposed by impurities. In the literature, the avalanche builds from initial carrier density of  $10^{11} - 10^{13} \text{ cm}^{-3}$ ; the calculations are not very sensitive due to uncertainties in  $\gamma$ .

We have no knowledge about calculations of pre-damage energy deposition using the avalanche model. But it was always assumed that this was the case, at least for material satisfying  $E_g/\hbar\omega \gg 1$ , and data from average samples supported this assumption

for alkali halide of four-photon band gap. Thus avalanche model calculations were concerned with deriving the break-down field,  $E_B$ , based on achieving carrier densities of  $n_c = 10^{18} \text{ cm}^{-3}$ , and not on what was happening before this threshold was reached.

### 4.2.3 Polaron Heating

In this model the electrons in the conduction band are strongly coupled to the phonon system, any energy absorbed from the photon field is instantly put on a into the lattice. The lattice heating due to photon absorption by conduction band carriers is

$$\rho c(dT/dt) = n_c \sigma_p F \hbar \omega \quad (4.6)$$

where  $\sigma_p$  is the absorption cross section for laser photons by the polarons, the rest of symbol have already been defined.

The cross section  $\sigma_p$  is an experimentally unmeasured quantity in NaCl at visible wavelengths of light.

Schmid et al.[5] used the theory of Pokatilov and Fomin for  $\sigma_p$  when they introduced the polaron heating model to the laser damage field. In this theory, the absorption cross section  $\sigma_p$  is dominated by interaction with acoustic phonons (the electron coupled to acoustic phonons may be called a polaron). The  $\sigma_p$  is calculated in equation,

$$\sigma_p \approx \left( 8\pi^2 e^2 / 3m\hbar\omega^2 n c_1 \right) \sqrt{(2\pi m / kT) \text{ Sinh}(\hbar\omega / 2kT)} \times (\hbar / 2m\omega)^{\mu-1} \{ 2K_{2-\mu}(\hbar\omega / 2kT) \} V \quad (4.7)$$

which is valid for the limit  $\hbar\omega/2kT \gg 1$  and  $\omega_0/\omega \ll 1$ , where  $\omega$  is the photon frequency and  $\omega_0$  is the highest phonon frequency of the scattering mechanism being considered.  $K_\nu$  is the modified Bessel function,  $c_1$  is light speed, and  $V$  corresponds to the matrix elements for the scattering mechanism.

For optical phonon scattering,

$$\mu=1 \quad \text{and} \quad V = \alpha(\hbar\omega_0)^{3/2} / \sqrt{2m\pi^2} \text{Sinh}(\hbar\omega_0 / 2kT) \quad (4.8)$$

and for acoustic phonon scattering,

$$\mu=1 \quad \text{and} \quad V = \varepsilon_j^2 kT / 4\pi^3 \hbar v_s^2 \quad (4.9)$$

where  $\alpha$  is the optical phonon coupling constant, for NaCl  $\alpha=5.5$ ,  $\varepsilon_j$  is the deformation potential, and for NaCl  $\varepsilon_j=8.9$  eV.

For optical phonon scattering, using the parameters given above,  $\sigma_{p(\text{opt})} \leq 7 \times 10^{-20}$   $\text{cm}^2$ , while for acoustic phonon scattering,  $\sigma_{p(\text{ac})} \approx 5.5 \times 10^{-19}$   $\text{cm}^2$  at 532 nm, and we used acoustic scattering in our calculations because of review of the literature, acoustic phonon scattering is the most effective mechanism for lattice heating, and the magnitude of the polaron absorption coefficient is variable but nearly  $\sigma_p \approx 5 \times 10^{-19}$   $\text{cm}^2$  (at 532 nm wavelength).

#### 4.2.4 Primary Defects

The energy to create an electron-hole pair ( $E_g$ ) can be regarded as an energy barrier to a whole host of processes. In the tight binding picture of energy bands in solids, appropriate for alkali halides, band gap excitation raises an electron from the highest occupied halogen p orbital to the lowest unoccupied alkali s orbital. In NaCl, this creates



a  $Cl^0$  atom and a "free" electron. The  $Cl^0$  bonds to nearest neighbor  $Cl^-$  in a  $\langle 110 \rangle$  direction, forming a  $Cl_2^-$  molecular ion in the lattice within  $10^{-13}$  sec[15]. This molecular ion can be considered as a trapped hole since there is a deficiency of negative charge localized on this ion, and is known as  $V_K$  center. The  $V_K$  center forms a region of positive charge that interacts with the free electron and there exist a series of one-electron levels superimposed on the crystal band structure. As the electron relaxes to the conduction band edge, it becomes bound to the  $V_K$  center and eventually relaxes to one of the levels in the gap if it does not recombine with the hole directly. When the electron occupies one of the levels in the gap associated with the  $V_K$  center, the system is known as a self-trapped exciton or STE, which is essentially a  $Cl_2^{--}$  ion. When the excited electron falls into the trapped hole the  $Cl_2^{--}$  ion has no yet bonding and dissociates into  $2Cl^-$ , returning the crystal ground state.

Alkali halides have characteristic luminescence due to relaxation of excited states of the STE. In NaCl there are two luminescence bands observable at temperatures below about 100K, one with a relatively long lifetime (on the order of one millisecond at low temperature), the other having a lifetime of about 1 nsec below 50 K [9]. The initial states of these transitions are known to be different excited states of the STE, both within the forbidden region of the ground state crystal. The duration of laser pulses  $\approx 85$  psec further can excite the STE from the state (term symbols, e.g.,  $^3\Sigma_u^+$  refer to STE only). Observed absorption bands due to STE-  $V_K$  transitions are believed to be the  $S_3 \rightarrow S^*$  electron transition (STE) and these two excited states, causing a redistribution of the relative populations and further energy transfer from the laser beam to the crystal. There are three excited states of STE with  $S^*$ ,  $S_1$ ,  $S_3$  see Figure 4.2. The state  $S_1$  is responsible for the short lifetime luminescence, and the state  $S_3$  is the initial state of the slow luminescence. The state  $S^*$  is a nonradiative excited state above both  $S_1$  and  $S_3$ .

In addition to these transient crystal "defects" band gap excitation in alkali halides is also known to lead to formation of F-H defect pairs. The F-center is a  $Cl^-$  vacancy

occupied by a single electron, while the H center is a  $Cl_2^-$  ion in the place of a single  $Cl^-$  ion. It was believed that the STE and the close F-H pair are isomers. The STE  $S_3$  state is really a nearest-neighbor F-H pair. There are more paths away from the F center for the H center to migrate, F-center yield increases with temperature while the recombination luminescence decreases.

NaCl does not exhibit efficient F-center formation at low temperatures. Since the review of literature considers the  $\pi$  luminescence to arise from e-h recombination in an STE, there is an absorption due to the  $V_K$  center, and is termed a hole transition. An electron from the valence band is elevated to the level of the unpaired electron of the  $V_K$  center, or, one can look at it as the hole going from the upper state to the lower state (see Figure 4.2). This hole absorption is characterized by a very broad absorption band in the near UV which also overlaps the wavelength laser photons, thus providing another channel for energy deposition. This hole absorption can also occur when the hole is associated with an STE. An  $S_3$  STE, the Auger transfer results in an  $S^*$  STE, since there is energy  $\hbar\omega$  available, while for  $S_1$  or  $S^*$  STEs, the Auger process results in ionization of the STE; i.e.,  $V_K +$  free electron.

The four-photon absorption is not only mechanism for energy deposition in the crystal. A kinetic model of the interaction of the transient and stable defects with photon field. The idea is to determine to what extent defects absorb energy and recycle among themselves before forming stable F-centers or disappear by way of e-h recombination. And also, the relative importance of each species to energy absorption can be determined. The model calculates the population of all species according to generation mechanisms given and the heating associated with their formation, relaxation, and annihilation.

Braunlich et al.[30] attempted to come up with a set of kinetic equations to calculate the role of primary defects in laser damage of NaCl specifically to determine how considering the effects of primary defects would alter the calculated damage threshold. This model was incomplete and contained several poor choices for values of

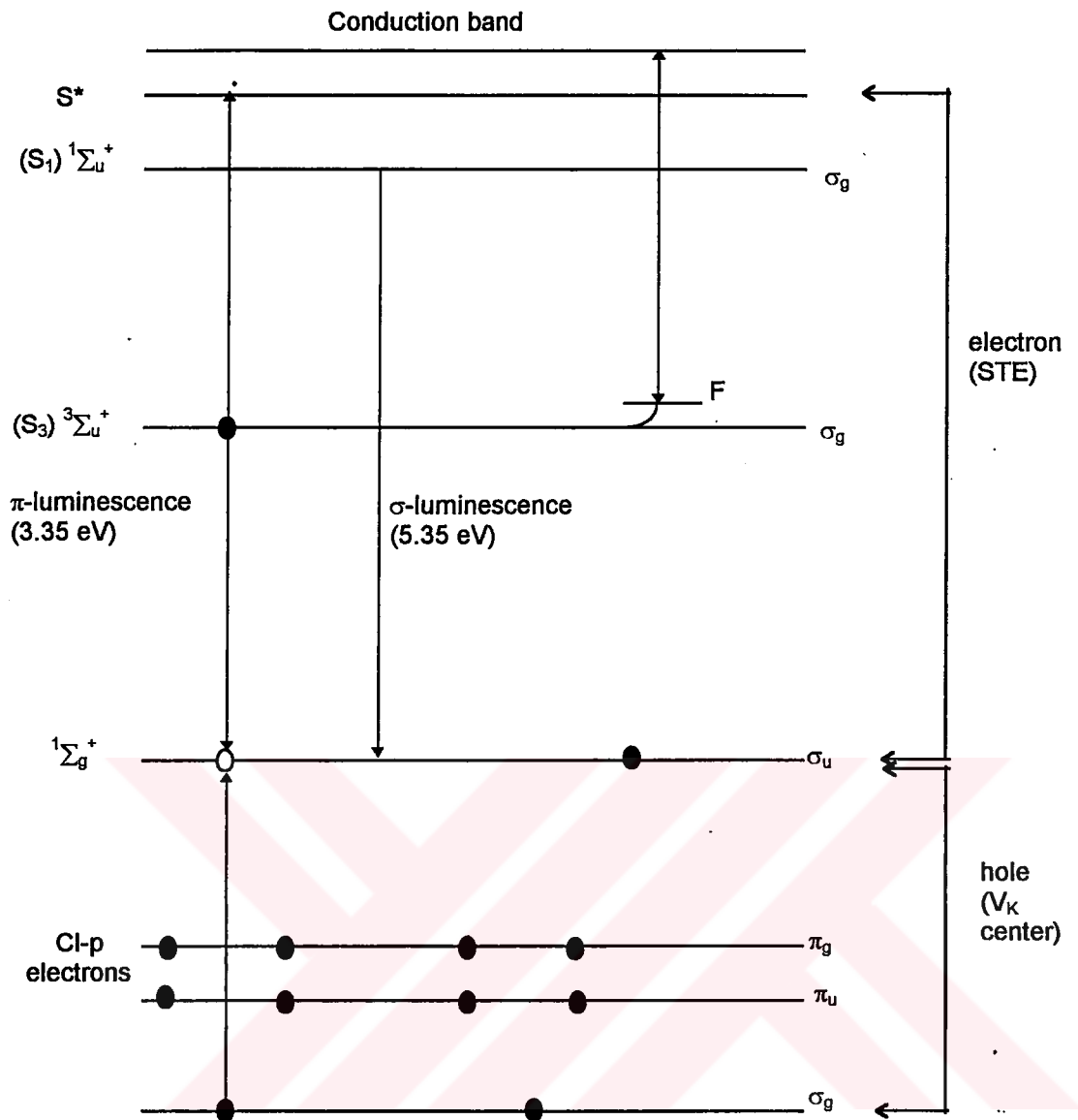


**Figure 4.2** Schematic energy level diagram of the  $V_K$  center and STE [9]. The orbitals are the molecular levels occupied by the eleven outer atomic chlorine p-electrons in the self-trapped hole or  $V_K$  center configuration ( $Cl_2^+$ ). The excited electron of the STE occupies either state  $1\Sigma_u^+(S_1)$  or  $3\Sigma_u^+(S_3)$  when trapped from the conduction band. Recombination with the hole from either state results in the luminescence labeled  $\sigma$  and  $\pi$  respectively, forms the dissociative  $1\Sigma_g^+$  STE  $\sigma_u \rightarrow \sigma_g$  hole transition (electron:  $\sigma_g \rightarrow \sigma_u$ ). some critical parameters. Braunlich et al. attempted to calculate the laser flux required to heat the crystal to the melting point, which is taken as the damage criterion.

The study of primary defects in alkali halides tends to span all of these materials. NaCl may be less well known than other alkali halides. All alkali halides do not behave identically to NaCl, and should avoid generalizing the more specific results to other alkali halides. Williams et al.[44] studied for understanding of primary defects in alkali halides, unfortunately, there was not much interest in obtaining absolute absorption coefficient either, as these are not necessary for interpreting absorption spectra.

#### 4.3 PARAMETERS OF THE PRIMARY DEFECT MODEL

The  $V_K$  center widely held to form in a time on the order of the period of the highest energy lattice mode,  $\approx 10^{-13}$  sec[15]. We have taken the cross section for capture of a polaron to be approximately  $4 \times 10^{-14}$  cm<sup>2</sup> based on the following due to Williams et al., the lifetime of a free carrier (density  $n_c$ ) to become trapped in a bimolecular kinetic model is  $\tau = (\sigma v n_c)^{-1}$ . The velocity  $v$  of a polaron is estimated from the excess kinetic energy ( $\approx \hbar \omega_{LO}$ ) of the polaron to be  $\approx 10^7$  cm/sec. With calculated carrier density of  $n_c = 5 \times 10^{17}$  cm<sup>-3</sup> and a measured  $\tau$  taken to be the buildup time of STE luminescence in NaCl of  $\cong 5$  psec.

$$\sigma = (\tau v n_c)^{-1} = 4 \times 10^{-14} \text{ cm}^2 \quad (4.10)$$

since  $V_K \approx n_c$ ,

$$\sigma = (\tau v V_K)^{-1}$$

Thus the capture of polarons by  $V_K$  centers

$$dn_c/dt = n_c/\tau = n_c \sigma v V_K,$$

where  $V_K$  is the density of  $V_K$  centers. The captured polarons has three possible branching. The first is direct e-h recombination, the other two are formation of STE states.

Figure 4.2 shows the relevant states of the STE. The  ${}^1\Sigma_g^+$  state is the ground state of the unstable  $Cl_2^-$  molecule. At low temperature, the transitions  ${}^3\Sigma_g^+ \rightarrow {}^1\Sigma_g^+$  and  ${}^1\Sigma_u^+ \rightarrow {}^1\Sigma_g^+$  give off the luminescence labeled  $\pi$  and  $\sigma$ , respectively. The state  $S^*$  is that reached when an  $S_3$  exciton absorbs a single 532 nm photon. However, the level occupied by the hole is not a well known quantity and we must estimate its level by considering energy balance in the overall interaction of the defects with the laser photons. In Figure 4.2, the  $V_K$  center absorption of 532 nm photons results in the electron transition  $\sigma_g \rightarrow \sigma_u$ . Note that this creates a condition of antibonding of the  $V_K$  center, thus it dissociates ( $\sigma_g$  and  $\pi_u$  orbitals are bonding,  $\sigma_u$  and  $\pi_g$  orbitals are antibonding, this is also why the center dissociates when the electron recombines with the  $\sigma_g$  hole in the STE, there is no net bonding). But  $V_K$  center reforms very rapidly and so the net effect of  $V_K$  absorption is dissipation of 2.33 eV (energy of 532 nm photon) to the lattice.

The  $\pi$  luminescence of 3.35 eV then placed the  $S_3$  level at  $\approx 2.9$  eV below the conduction band, [16]. The state  $S_1$  is 5.35 eV above the hole level or,  $\approx 0.9$  eV below the conduction band and  $S^*$  is 2.33 eV above  $S_3$  or  $\approx 0.6$  eV below the conduction band. It turns out that the precise placement of these levels is not critical in the heating calculation.

At low temperatures William et al. [15] measured yield of  $S_3$  STE's in NaCl following 9.32 eV excitation and found 0.19  $S_3$  STEs per e-h pair created at 15 K. Ikezawa and Kojima measured the luminescence spectrum of NaCl at 11K. The  $\pi$  and  $\sigma$  bands fit Gaussian curves very well, by calculating the areas under the  $\pi$  and  $\sigma$  bands, a formation ratio of  $S_1/S_3 \cong 0.13$ , assuming that at low temperatures e-h recombination is 100 percent radiative from the  $S_1$  and  $S_3$  STE states.

The fraction of polarons captured by  $V_K$  centers that fall into each of three channels: a fraction  $B_p = 0.785$  of captured polarons recombine nonradiatively directly

with self trapped holes,  $B_3 = 0.19$  polarons combine with the  $V_K$  center to form a  $S_3$  STE and  $B_1 = 0.025$  from the  $S_1$  STE states[9].

The single 532 nm photon absorption by  $S_3$  STEs creates an  $S^*$  exciton. Exciton state absorption experiments by Soda and Itoh [33] in NaCl at 5K found that 97 percent of the  $S^*$  excitons created by 2.33 eV excitation of  $S_3$  excitons relaxed back to the  $S_3$  state, while the conversion to both  $\sigma$  luminescence and F centers combined occurs for about three percent of  $S^*$ , in the ratio  $\sigma/F = 9/1$ . The branching  $S_3:S_1:F = 0.97:0.027:0.03$  is highly wavelength dependent.

If the  $V_K$  center absorb polarized light, an effect known as dichroic bleaching or optical reorientation occurs. Hole absorption results in dissociation of the  $V_K$  center, and subsequent reorientation is equally probable along the six equivalent  $[110]$  directions. The  $V_K$  center must be considered three subspecies  $V_{K1}$  has bond axis parallel to  $\langle 110 \rangle$ ,  $V_{K2}$  has axis at angle to  $\langle 110 \rangle$ , that is, axis is parallel to  $\langle 101 \rangle$ ,  $\langle 10\bar{1} \rangle$ ,  $\langle 011 \rangle$ , or  $\langle 0\bar{1}1 \rangle$ , and  $V_{K3}$  is perpendicular to  $\langle 110 \rangle$ ; i.e., parallel  $\langle \bar{1}\bar{1}0 \rangle$ . For light parallel to  $\langle 110 \rangle$ , the hole absorption should be approximately four times stronger for  $V_{K1}$  centers than for  $V_{K2}$  centers.

The only real room temperature data are the STE $\rightarrow$ F conversion, STE absorption rise time (5psec), and F-center properties.

#### 4.4 MODEL EQUATIONS

There are three different models in order to calculate the focal point temperature increase  $\Delta T_0$  versus peak laser flux,  $F_p$ . These are

- a) multiphoton-polaron-defect heating
- b) multiphoton-assisted avalanche heating

c) avalanche only

In model a) Jones [9] exchanges free and polaron heating terms;  $A^* = \sigma^{(4)} N F^4$ . In model b) multiphoton free-carrier generation provides starting electrons for the avalanche;  $A^* = \sigma^{(4)} N F^4 + \gamma n_c$  and in model c) they assumed a starting density  $n_{c0}$ ;  $A^* = \gamma n_c$ .

The rate equations are obtained by Braunlich et al., (1981)[30] as in below

$$\begin{aligned} \frac{dn_c}{dt} &= \sigma^{(4)} F^4 n_v \\ \frac{dp}{dt} &= \sigma^{(4)} F^4 n_v - p \tau_{VK}^{-1} + F \sigma_{VK} V_K \\ V_K &= n_c - p \\ n_v &= N_V - p. \end{aligned} \quad (4.11)$$

Where  $n_c$ ,  $n_v$ ,  $p$ ,  $V_K$ ,  $\tau_{VK}$ ,  $\sigma_{VK}$ ,  $F$ ,  $\sigma^{(4)}$ , free carrier density, concentration of electrons in the CB, concentration of valance electrons, concentration of free holes, concentration of  $V_K$ -center, lifetime of a free hole, cross section for photon absorption by and dissociation of a  $V_K$ -center, photon flux, four-photon cross sections respectively. But they not obtained the value of four cross section in experimentally.

Then, a large set of coupled differential equations for the concentrations of the various species ( $n_c$ ,  $p$ ,  $V_K$ -centers, self trapped excitons, F-center density) and the increase in lattice temperature are derived by Jones et al. [9] and they obtained four-photon cross section in experimentally. The kinetic equations and its terms are listed Table 2 and Table 3 respectively. They included the probability  $\beta$  for free electron capture by ionized F-center ( $CI$  vacancies) denoted as  $F^+$  centers. Free holes, concentration  $p$ , are created when an electron is excited from the valance band and also when a  $V_K$  center is dissociated by hole absorption. The energy dissipated in the lattice by hole trapping appears as  $(p/\tau_{VK})E_{VK}$ .

For computational convenience, the laser pulse is taken as

$$F(t) = F_p \exp\{-(t/\tau) - \sqrt{5} \}^2 \} [9]. \quad (4.12)$$

where  $F(t)$  laser pulse is dependent on time,  $F_p$  is  $1.34 \times 10^{30}$  photons/cm<sup>2</sup> sec,  $t$  is time,  $\tau$  is 85 psec and calculation begins at  $t = 0$  and  $t = 190$  psec.

#### a) Multiphoton Polaron Model

In this model, only hole absorption, direct e-h recombination and polaron absorption contribute to heating, with other species contributing much less.

Jones et al.[9] showed there is no big difference in exchanging free carrier and polaron heating term, they obtained the same slope to draw photon-flux versus temperature.  $\sigma^{(4)} = 2 \times 10^{-113} \text{ cm}^8 \text{ sec}^3$  with slope  $\approx 3.7$  for polaron defect,  $\sigma^{(4)} = 1.5 \times 10^{-114} \text{ cm}^8 \text{ sec}^3$  with slope  $\approx 3.9$  for free electron defect. Figure 4.3 show the conduction band carrier concentration[9]. So we take  $\sigma^{(4)} = 2 \times 10^{-113} \text{ cm}^8 \text{ sec}^3$  and  $\sigma^{(4)} = 1.5 \times 10^{-114} \text{ cm}^8 \text{ sec}^3$  for solving kinetic equation.

#### b) Multiphoton- assisted avalanche heating with free-electron heating

In this model we could not find any experimental data. Since, no value of the parameter  $a$  in the range  $3 \times 10^{-17} \leq a \leq 1 \times 10^{-5}$  could account for the experimental data.

#### c) Avalanche e-h generation-free carrier heating model

The model with avalanche carrier generation is the only mechanism for valance excitation. The avalanche mechanism plays no role in carrier generation up to temperatures[9] they have obtained. It is clear that it would be nearly impossible to



measure predamage energy deposition if it were due to avalanche generation. Review of literature, nobody to measure melting point, so nobody conclude with certainty that avalanche formation does not occur or play a role in laser damage. The avalanche mechanism is invoked to explain the threshold aspect of intrinsic laser damage.

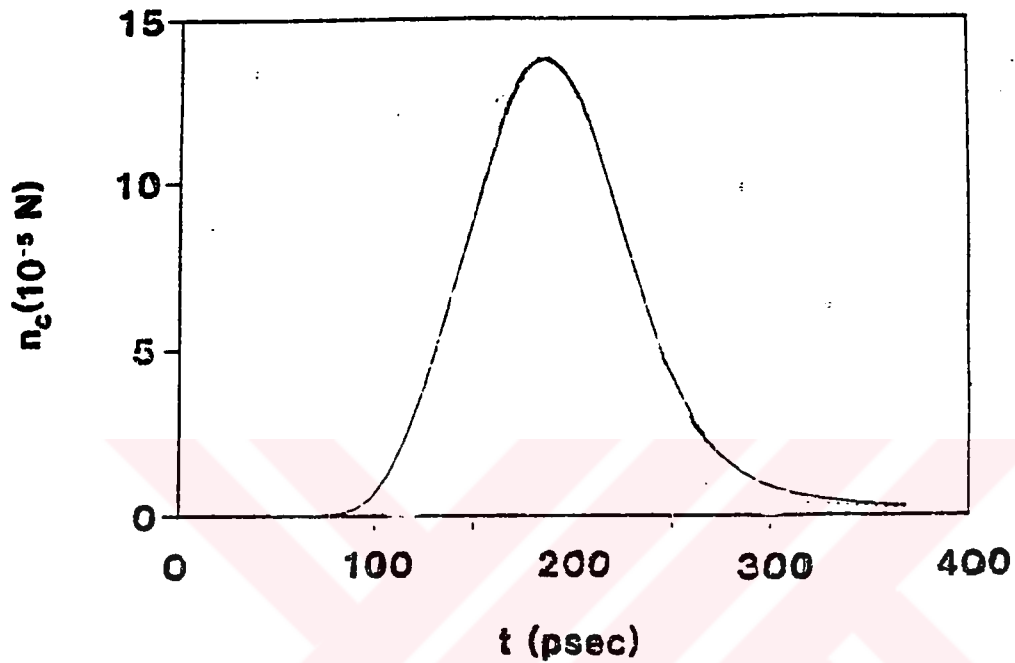


**Figure 4.3** Free-carrier density, in terms of the density of active atoms,  $N= 2.2 \times 10^{22} \text{ cm}^{-3}$  [9].

**TABLE 2 KINETIC EQUATIONS**

$$\frac{dn_c}{dt} = A^* - \sigma n_c \nu V_K + \sigma_h (S_1 + S^*) F + \sigma_{s^*} S^* F + \sigma_{s_1} S_1 F + \sigma_F n_F F - \beta n^+ n_c$$

$$\frac{dp}{dt} = A^* - p / \tau_{VK} + 4\sigma_h V_{K1} F + \sigma_h V_{K2} F$$

$$\frac{dV_{K1}}{dt} = \frac{1}{6} \frac{p}{\tau_{VK}} - \gamma_0 \sigma n_c \nu V_{K1} + \left(\frac{1}{6}\right) (\sigma_h + \sigma_{s^*}) S^* F + \frac{1}{6} (\sigma_h + \sigma_{s_1}) S_1 F - 4\sigma_h V_{K1} F$$

$$\frac{dV_{K2}}{dt} = \frac{4}{6} \frac{p}{\tau_{VK}} - \gamma_0 \sigma n_c \nu V_{K2} + \left(\frac{4}{6}\right) (\sigma_h + \sigma_{s^*}) S^* F + \frac{4}{6} (\sigma_h + \sigma_{s_1}) S_1 F - \sigma_h V_{K2} F$$

$$\frac{dV_{K3}}{dt} = \frac{1}{6} \frac{p}{\tau_{VK}} - \gamma_0 \sigma n_c \nu V_{K3} + \left(\frac{1}{6}\right) (\sigma_h + \sigma_{s^*}) S^* F + \frac{1}{6} (\sigma_h + \sigma_{s_1}) S_1 F$$

$$\frac{dS^*}{dt} = (\sigma_h + \sigma_{s_3}) S_3 F - (\sigma_h + \sigma_{s^*}) S^* F - \frac{S^*}{\tau_{s^*}}$$

$$\frac{dS_1}{dt} = \gamma_1 \sigma n_c \nu V_K - (\sigma_h + \sigma_{s_1}) S_1 F + \eta_1 \frac{S^*}{\tau_{s^*}} - \frac{S_1}{\tau_{s_1}}$$

$$\frac{dS_3}{dt} = \gamma_3 \sigma n_c \nu V_K + -(\sigma_h + \sigma_{s_3}) S_3 F + \eta_3 \frac{S^*}{\tau_{s^*}} - \frac{S_3}{\tau_F}$$

$$\frac{dn_F}{dt} = \frac{S_3}{\tau_F} + n_c \beta n^+ + \eta_F \frac{S^*}{\tau_{s^*}} - \sigma_F n_F F$$

$$\frac{dn_F^+}{dt} = \sigma_F n_F F - n_c \beta n^+$$

$$\begin{aligned} \rho c \frac{dT}{dt} = & B^* + \sigma n_c \nu V_K \left[ \gamma_0 (E_g - E_{VK}) + \gamma_1 E_{s_1} + \gamma_3 E_{s_3} \right] \\ & + (p / \tau_{VK}) E_{VK} + (\sigma_h + \sigma_{s^*}) S^* F (h\nu - E_{s^*}) + (\sigma_h + \sigma_{s_1}) S_1 F (h\nu - E_{s_1}) \\ & + \eta_3 (S^* / \tau_{s^*}) h\nu + \eta_1 (S^* / \tau_{s^*}) (E_{s_1} - E_{s^*}) + \eta_F (S^* / \tau_{s^*}) h\nu \\ & + (S_1 / \tau_{s_1}) (E_g - E_{s_1} - E_{VK}) + \beta n_c n^+ E_F \end{aligned}$$

**TABLE 3 DEFINITION AND VALUE OF PARAMETERS IN TABLE 2**

$n_c$	Conduction band carrier concentration
$p$	Free-hole density
$V_{k1}$	Density of $V_k$ centers parallel to [110] laser polarization
$V_{k2}$	Density of $V_k$ centers at angle to [110]
$V_{k3}$	Density of $V_k$ centers oriented perpendicular to [110]
$S_1$	Density of STE's in singlet state $S_1$
$S_3$	Density of STE's in triplet state $S_3$
$S^*$	Density of STE's in higher excited state $S^*$
$n_F$	F-center density
$N=2.23 \times 10^{22} \text{ cm}^{-3}$	Density of active atoms
$F$	Photon flux in photons/cm <sup>2</sup> sec
$\tau_{VK} \approx 10^{-13} \text{ sec}$	Formation time of $V_K$ -center [15]
$\tau_{S1} = 8 \times 10^{-12} \text{ sec}$	Nonradiative lifetime of $S_1$ STE [45]
$\tau_F = 815 \times 10^{-12} \text{ sec}$	Nonradiative lifetime of $S_3 \rightarrow$ F-center conversion [20]
$\tau_{S^*} = 5 \times 10^{-12} \text{ sec}$	Nonradiative lifetime of $S^*$ STE
$\sigma = 4 \times 10^{-14} \text{ cm}^2$	Cross section for capture of free carrier by $V_K$ [15]
$\sigma_h = 8.6 \times 10^{-18} \text{ cm}^2$	Cross section of Single photon absorption for trapped holes at 532 nm [16]
$\sigma_{S^*} = 5 \times 10^{-17} \text{ cm}^2$	Absorption cross section for $S^*$ STE at 532 nm [9]
$\sigma_{S1} = 5 \times 10^{-17} \text{ cm}^2$	Absorption cross section for $S_1$ STE at 532 nm [9]
$\sigma_{S3} = 1.2 \times 10^{-16} \text{ cm}^2$	Absorption cross section for $S_3$ STE at 532 nm [16]
$\sigma_F = 5 \times 10^{-17} \text{ cm}^2$	Absorption cross section for F STE at 532 nm
$\beta = 1.45 \times 10^{-6} \text{ cm}^3/\text{sec}$	Probability for ionized F center to capture free carrier [4]
$\gamma_0 = 0.785$	Branching fraction for direct recombination of e-h

$\gamma_1 = 0.025$	Branching fraction for $S_1$ STE formation
$\gamma_3 = 0.19$	Branching fraction for $S_3$ STE formation [15]
$\eta_1 = 0.027$	Branching fraction of $S^* \rightarrow S_1$ [33]
$\eta_3 = 0.97$	Branching fraction of $S^* \rightarrow S_3$ [33]
$\eta_F = 0.003$	Branching fraction of $S^* \rightarrow$ F-center [33]
$v \approx 10^7$ cm/sec	Free- carrier velocity [9]
$E_g = 8.6$ eV	Energy gap of NaCl
$E_{S_1} = 0.9$ eV	Depth of $S_1$ state below conduction band [9]
$E_{S_3} = 2.9$ eV	Depth of $S_3$ state below conduction band [9]
$E_{S^*} = 0.6$ eV	Depth of $S^*$ state below conduction band [9]
$E_{V_K} = 2.33$ eV	Energy given to lattice when $V_K$ bond forms [9]
$E_F = 2.76$ eV	Depth of F center below conduction band [9]
$h\nu = 2.33$ eV	Photon energy at 532 nm
$\sigma_p \approx 5.5 \times 10^{-19}$ cm <sup>2</sup>	Polaron absorption cross section at 532 nm [5]
$A^* = \sigma^{(4)} N F^4$	In multiphoton-polaron model
$A^* = \sigma^{(4)} N F^4 + \gamma n_c$	In multiphoton-assisted avalanche model
$A^* = \gamma n_c$	In avalanche only model.
$B^* = \sigma^{(4)} N F^4 (4h\nu - E_g)$	In multiphoton-polaron model
$+ \sigma_p n_c F h\nu$	In multiphoton-free electron heating, multiphoton assisted avalanche, and avalanche-only models.

# CHAPTER 5

## THE SOLUTION OF KINETIC EQUATIONS

### 5.1 INTRODUCTION

A response of alkali halide crystals to the generation of electron-hole pairs is the formation of such primary defects as  $V_K$ , F- and H centers and self-trapped excitons. The behavior of these nonequilibrium carriers and their concentration in pure NaCl crystal has been studied in terms of kinetic model of four-photon laser excitation and solved numerically.

Our aim was to examine computer simulation of the intrinsic behavior of NaCl in order to find the concentration of primary defects such as, F-,  $V_K$  center, STE, conduction band carrier concentration, free-hole density.

Jones et al.[9] showed that, four-photon absorption was the sole mechanism for e-h pair generation in intrinsic NaCl crystal, and they obtained four-photon cross section experimentally in the range  $1 \times 10^{-114} \text{ cm}^8 \text{ sec}^3 \leq \sigma^{(4)} \leq 20 \times 10^{-114} \text{ cm}^8 \text{ sec}^3$ . This range comes from the different boule of the NaCl crystal.

In the polaron-defect model, heating is dominated by hole absorption, followed by direct e-h recombination and finally polaron absorption, all other terms in the heating equation being negligible.

In the free carrier-defect, heating is completely dominated by the free carrier heating term, all others making up the small difference between the total temperature increase and the free carrier contribution.

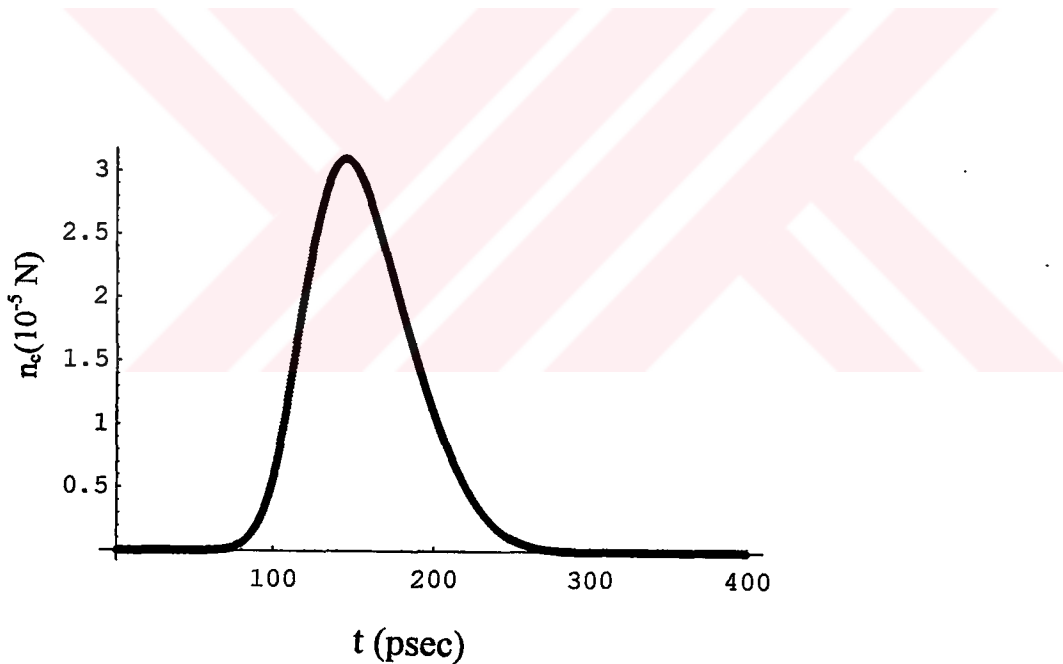
In this study we obtained concentration curves with the  $\sigma^{(4)} = 2 \times 10^{-113} \text{ cm}^8 \text{ sec}^3$  for multiphoton-polaron-defect model,  $\sigma^{(4)} = 1.5 \times 10^{-114} \text{ cm}^8 \text{ sec}^3$  for multiphoton-assisted-avalanche model. The other experimental values obtained from literature is seen in Table 3. The pulse is expressed as  $F(t) = F_p \exp\{-[(t/\tau) - \sqrt{5}]^2\}$ , the calculation begins at  $t = 0$  and the pulse peaks at  $t = 190 \text{ psec}$  for  $\tau = 85 \text{ psec}$ . And all concentrations are expressed in terms of the density of active ions ( $CI$ ),  $N = 2.2 \times 10^{22} \text{ cm}^{-3}$ . The temperature are expressed in Kelvin and the starting temperature is  $293\text{K}$ . We have solved the kinetic equations (in Table 2) due to the multiphoton-polaron-defect heating model and multiphoton-assisted avalanche heating explained in Chapter 4 using the Runge Kutta method. The flowchart of computer programming is given in Appendix .

Figure 5.1 and 5.2 represents the conduction carrier and free holes densities  $n_c$  and  $p$  respectively as a function of polaron model,  $\sigma^{(4)} = 2 \times 10^{-113} \text{ cm}^8 \text{ sec}^3$ . The maximum concentrations are  $n_{c\text{max}} = 0.7 \times 10^{18} \text{ cm}^{-3}$  and  $p_{\text{max}} = 1 \times 10^{18} \text{ cm}^{-3}$  respectively from the Figures 5.1 and 5.2. The calculated concentration of  $V_{K1^-}$ ,  $V_{K2^-}$ , and  $V_{K3^-}$ , centers are shown in Figures 4.3, 4.4, 4.5, respectively. The maximum peak concentrations of  $V_{K1^-}$ , and  $V_{K2^-}$  centers are  $3.85 \times 10^{16}$  and  $5 \times 10^{18} \text{ cm}^{-3}$  respectively for the polaron model. These results clearly show the optical alignment of  $V_K$ -centers. The self-trapped exciton concentrations are plotted in Figures 5.6, 5.7, 5.8, for  $S_1$ ,  $S^*$ , and  $S_3$ , concentrations respectively. The STEs contribute negligibly to heating in both models. In polaron heating the STE concentrations have maxima at the flux peak of  $4.4 \times 10^{15}$ ,  $5.8 \times 10^{15}$ ,

$2 \times 10^{14}$ ,  $\text{cm}^{-3}$  for  $S_1$ ,  $S^*$ , and  $S_3$  respectively. The concentration of  $n_F$  and  $n_{F'}$  are shown in Figure 5.9 and 5.10, and concentration of  $n_F$  is  $1.7 \times 10^{12} \text{ cm}^{-3}$ .

We also solved rate equations for three values of peak flux  $F_p$  ( $F_{p1} = 1.343$  photons/ $\text{cm}^3\text{sec}$ ,  $F_{p2} = 5.343$  photons/ $\text{cm}^3\text{sec}$ ,  $F_{p3} = 7.343$  photons/ $\text{cm}^3\text{sec}$ ) corresponding to  $\sigma^{(4)} = 2 \times 10^{-113} \text{ cm}^8\text{sec}^3$  and  $\sigma^{(4)} = 3 \times 10^{-113} \text{ cm}^8\text{sec}^3$ , to obtain concentration of the free carrier density  $n_c$  as seen in Figure 5.11 and 5.12.

The calculation with multiphoton assisted avalanche model,  $\sigma^{(4)} = 1.5 \times 10^{-114} \text{ cm}^8\text{sec}^3$ , the concentration of species are so small as shown in Figures 5.13 to 5.22 due to heating the crystal may be damaged with avalanche free carrier.



**Figure 5.1** Free carrier density, in terms of the density of active atoms,  $N = 2.2 \times 10^{22} \text{ cm}^{-3}$  (for polaron model).

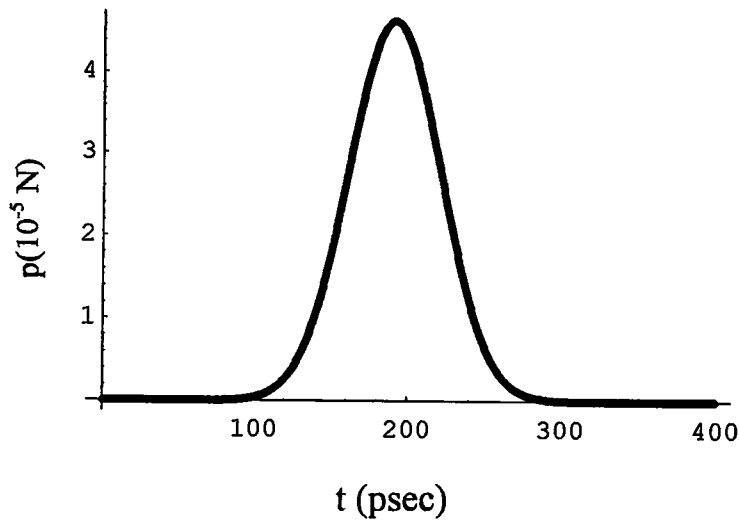


**Figure 5.2** Free hole density in terms of the density of active atoms,  $N = 2.2 \times 10^{22} \text{ cm}^{-3}$  (for polaron model).

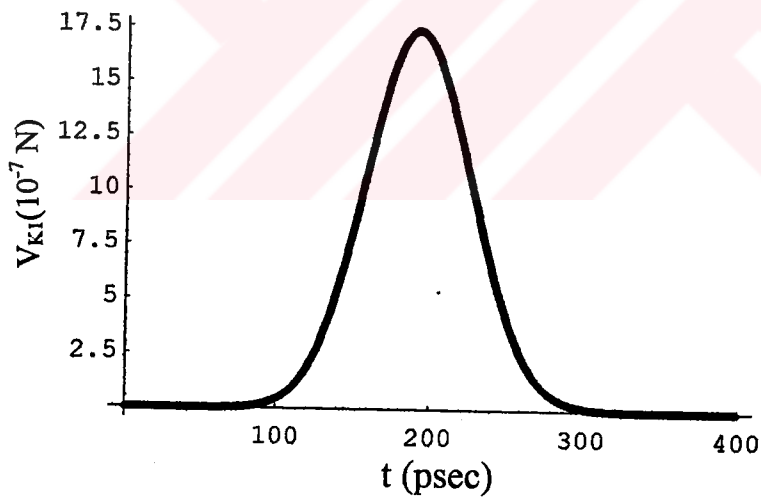


**Figure 5.3** Density of  $V_{KI}$ -centers in terms of the density of active atoms,  $N = 2.2 \times 10^{22} \text{ cm}^{-3}$  (for polaron model).



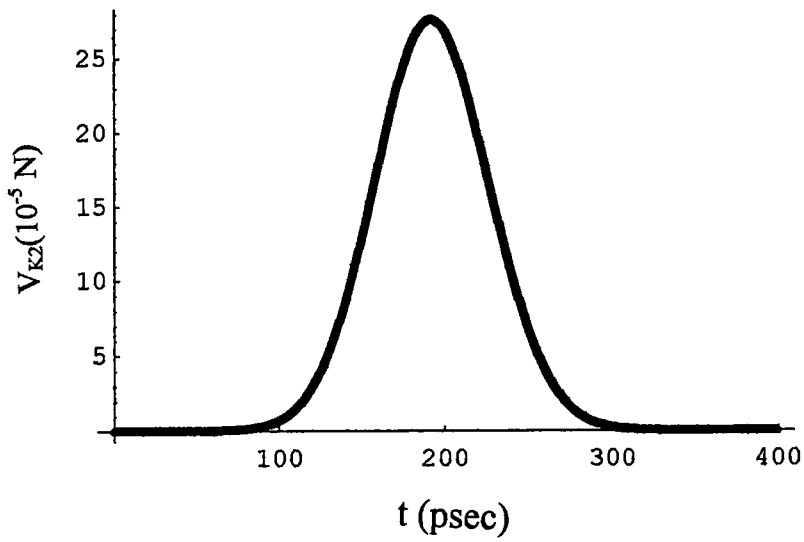


**Figure 5.4** Density of  $V_{K2}$ -centers in terms of the density of active atoms,  $N = 2.2 \times 10^{22} \text{ cm}^{-3}$  (for polaron model).

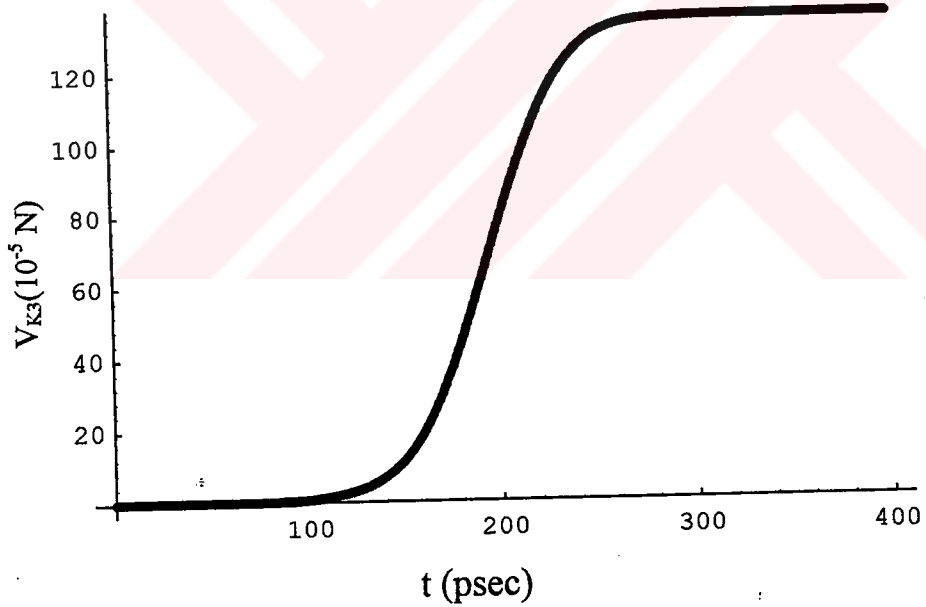


**Figure 5.5** Density of  $V_{K3}$ -centers in terms of the density of active atoms,  $N = 2.2 \times 10^{22} \text{ cm}^{-3}$  (for polaron model).

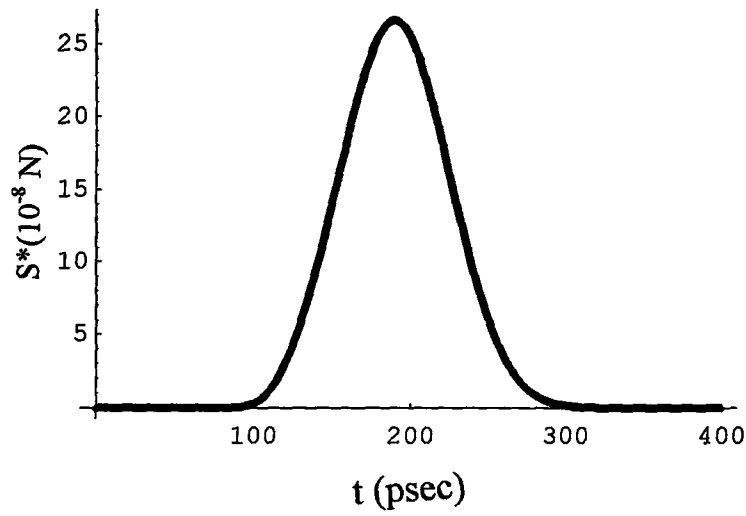


**Figure 5.6** Density of STEs in excited state  $S^*$  in terms of the density of active atoms,  $N = 2.2 \times 10^{22} \text{ cm}^{-3}$  (for polaron model).

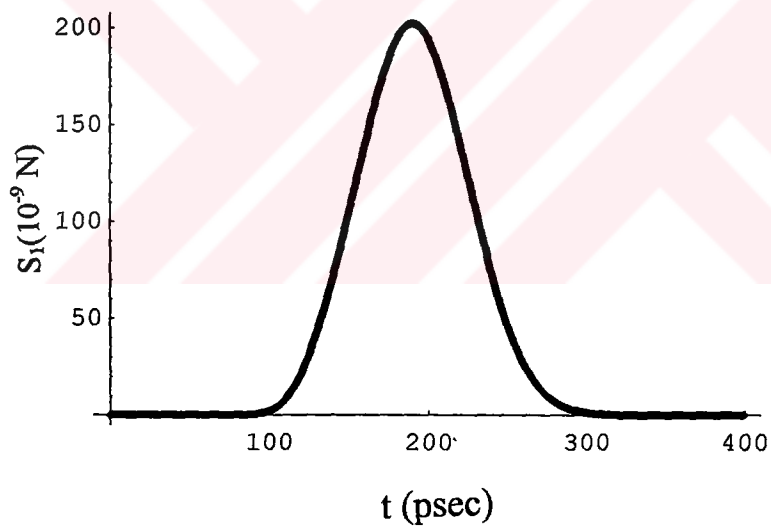


**Figure 5.7** Density of STEs in excited state  $S_1$  in terms of the density of active atoms,  $N = 2.2 \times 10^{22} \text{ cm}^{-3}$  (for polaron model).

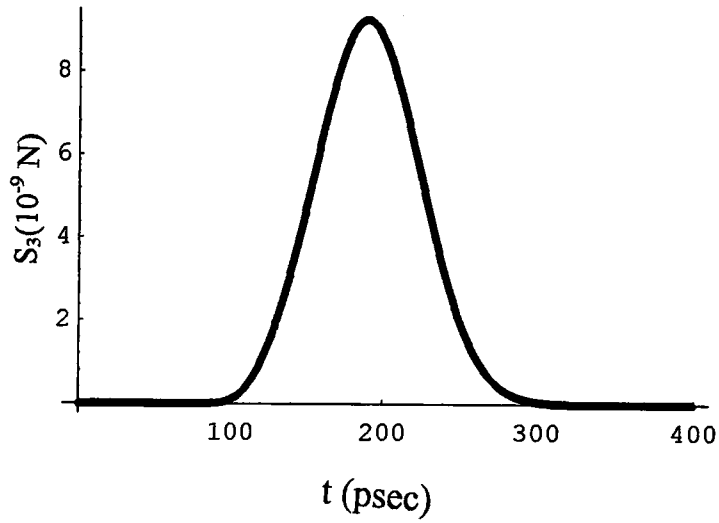


**Figure 5.8** Density of STEs in excited state  $S_3$  in terms of the density of active atoms,  $N = 2.2 \times 10^{22} \text{ cm}^{-3}$  (for polaron model).

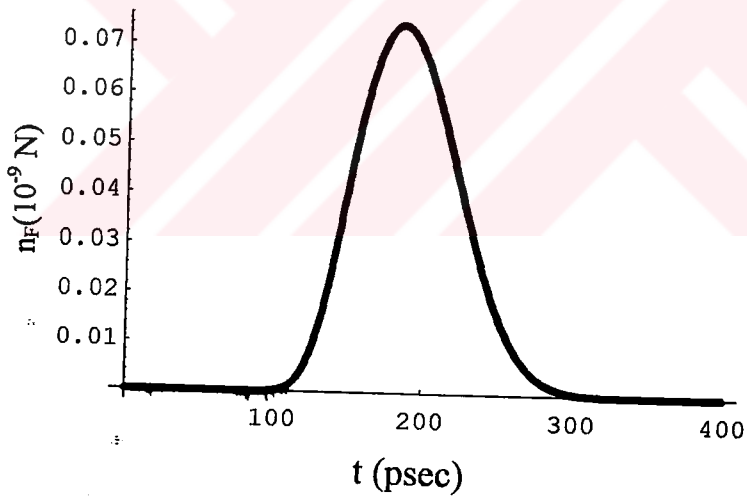


**Figure 5.9** Density of F-centers in terms of the density of active atoms,  $N = 2.2 \times 10^{22} \text{ cm}^{-3}$  (for polaron model).

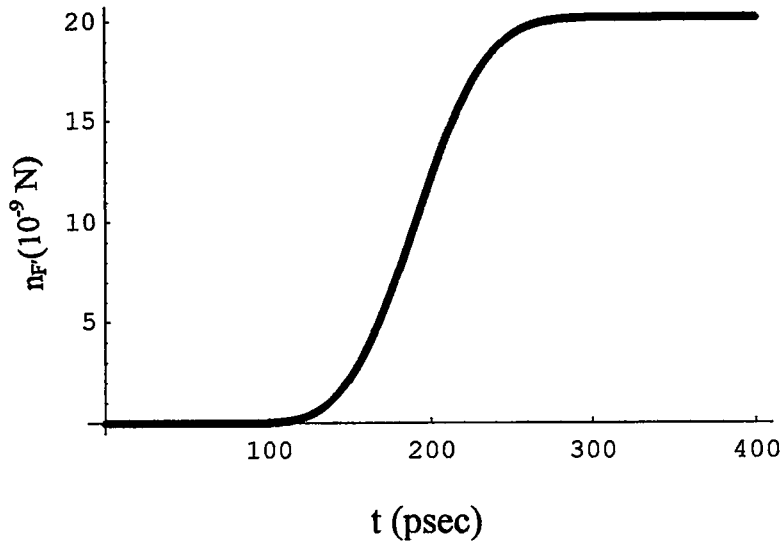


**Figure 5.10** Density of F<sup>2</sup>-centers in terms of the density of active atoms,  $N = 2.2 \times 10^{22} \text{ cm}^{-3}$  (for polaron model).

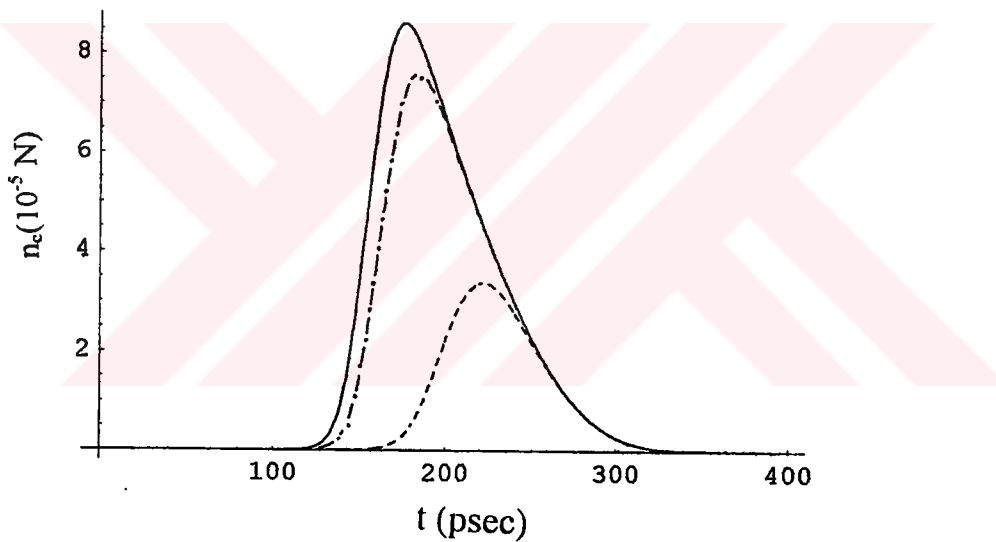


**Figure 5.11** Free carrier density with  $\sigma^{(4)} = 2 \times 10^{-113} \text{ cm}^8 \text{ sec}^3$ , dashed line for  $F_p = 1.343 \text{ photons/cm}^3 \text{ sec}$ , broken line for  $F_p = 5.343 \text{ photons/cm}^3 \text{ sec}$ , solid line for  $F_p = 7.343 \text{ photons/cm}^3 \text{ sec}$

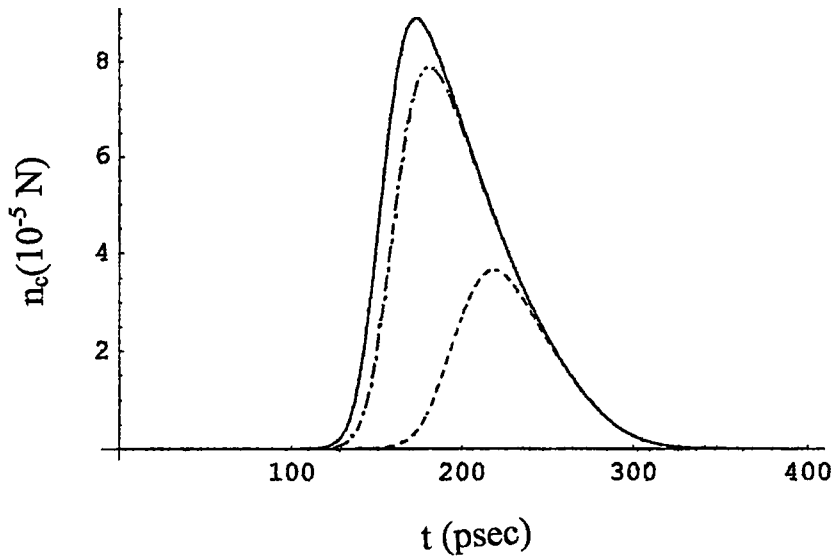


**Figure 5.12** Free carrier density with  $\sigma^{(4)}=3 \times 10^{-113} \text{ cm}^8 \text{ sec}^3$  dashed line for  $F_p=1.343 \text{ photons/cm}^3 \text{ sec}$ , broken line for  $F_p=5.343 \text{ photons/cm}^3 \text{ sec}$ , solid line for  $F_p=7.343 \text{ photons/cm}^3 \text{ sec}$

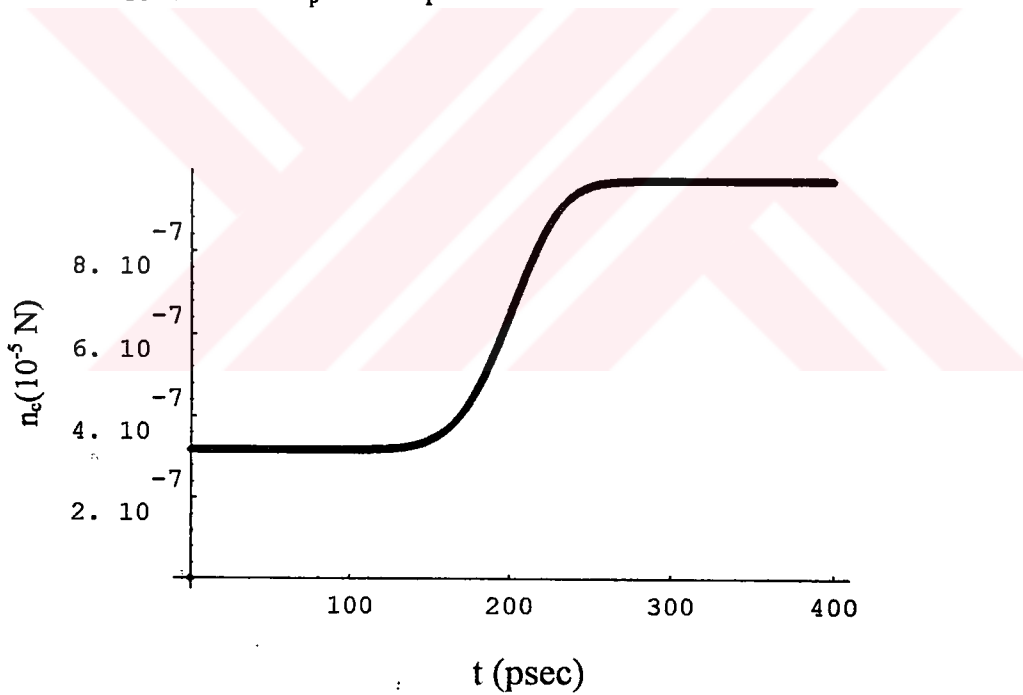


**Figure 5.13** Density of free carriers,  $n_c$ , with multiphoton-assisted-avalanche model.

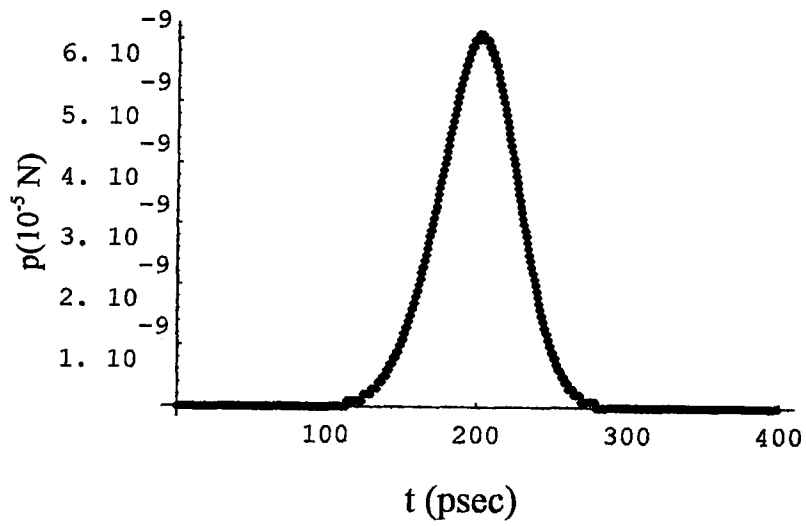


**Figure 5.14** Density of free holes,  $p$ , with multiphoton-assisted-avalanche model.

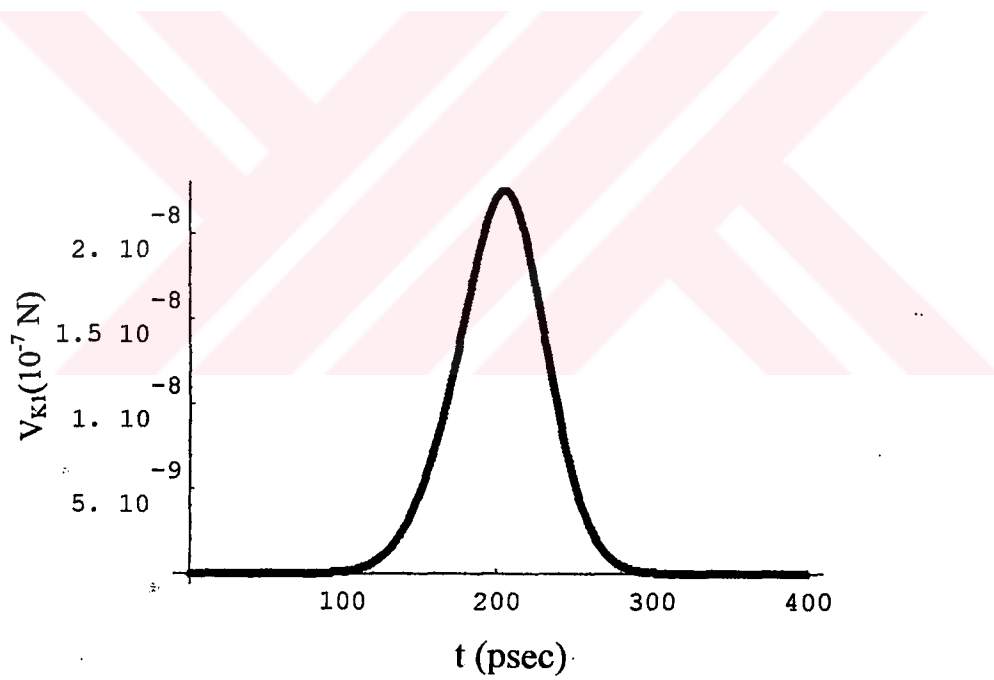


**Figure 5.15** Density of  $V_{K1}$ , with multiphoton-assisted-avalanche model.

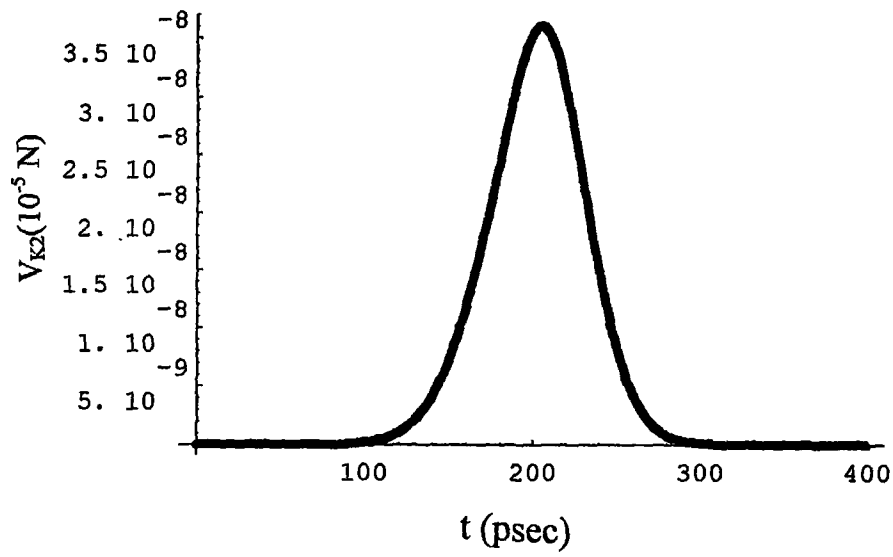


Figure 5.16 Density of  $V_{k2}$ , with multiphoton-assisted-avalanche model.

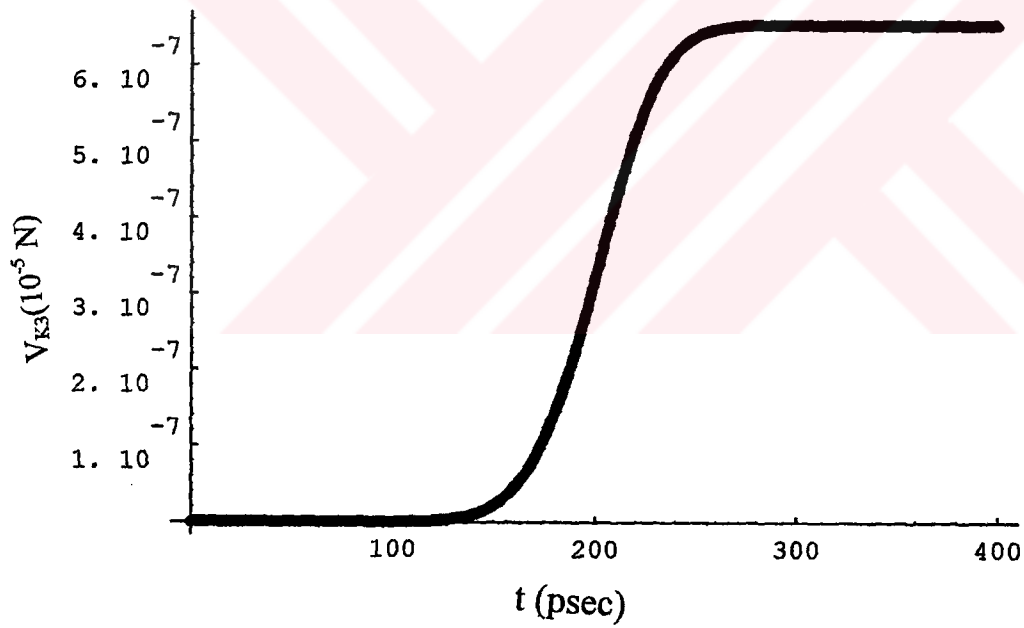
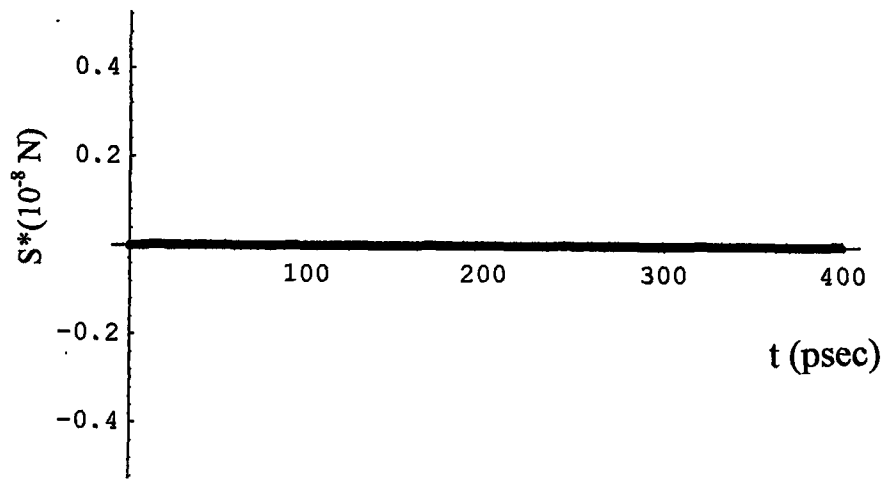
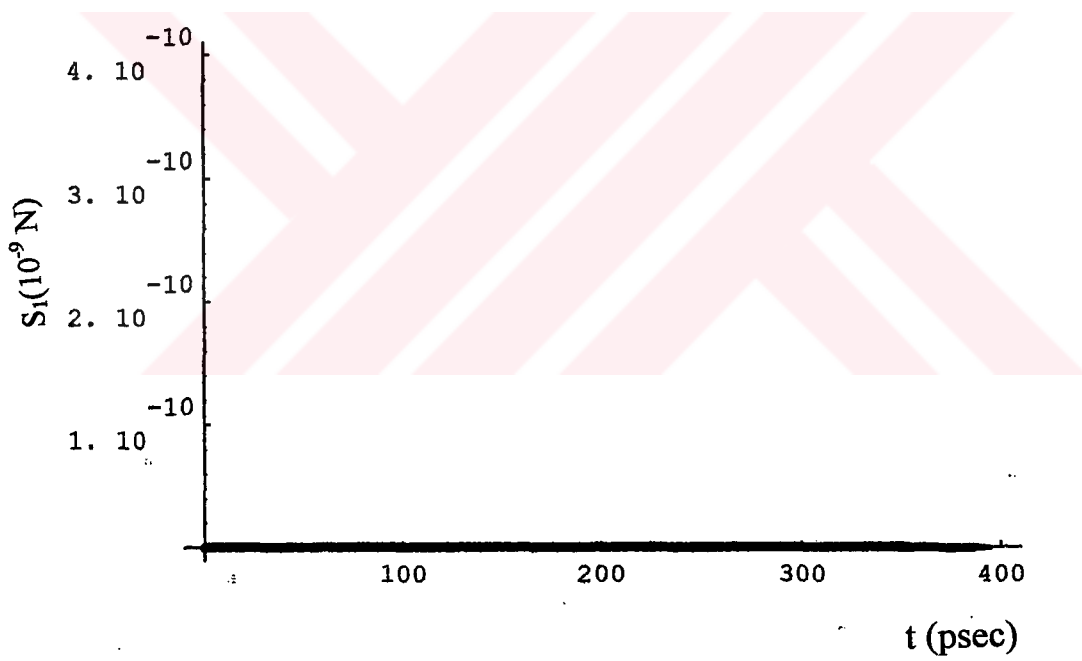


Figure 5.17 Density of  $V_{k3}$ , with multiphoton-assisted-avalanche model.



**Figure 5.18** Density of  $S^*$ , with multiphoton-assisted-avalanche model.



**Figure 5.19** Density of  $S_1$ , with multiphoton-assisted-avalanche model.



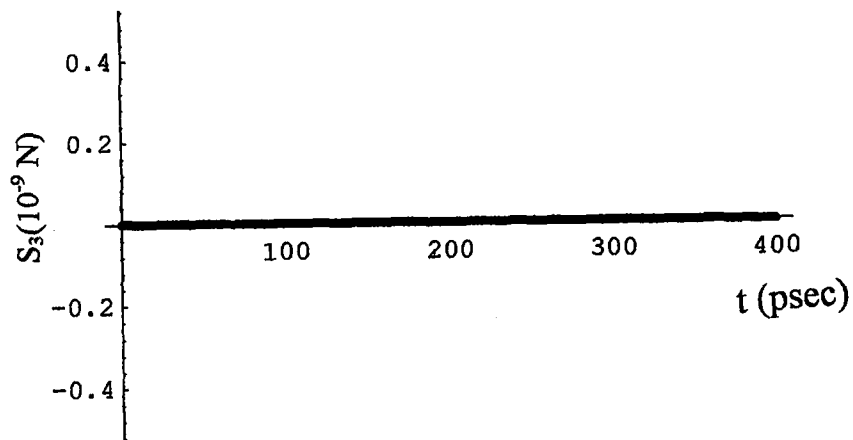


**Figure 5.20** Density of  $S_3$ , with multiphoton-assisted-avalanche model.

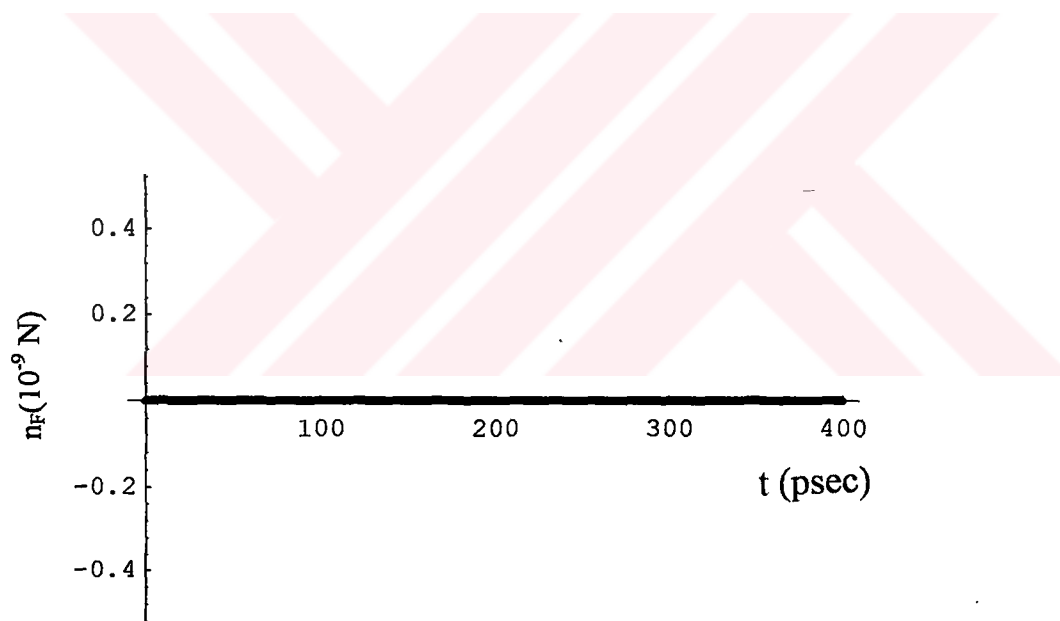


**Figure 5.21** Density of F-center,  $n_F$ , with multiphoton-assisted-avalanche model.

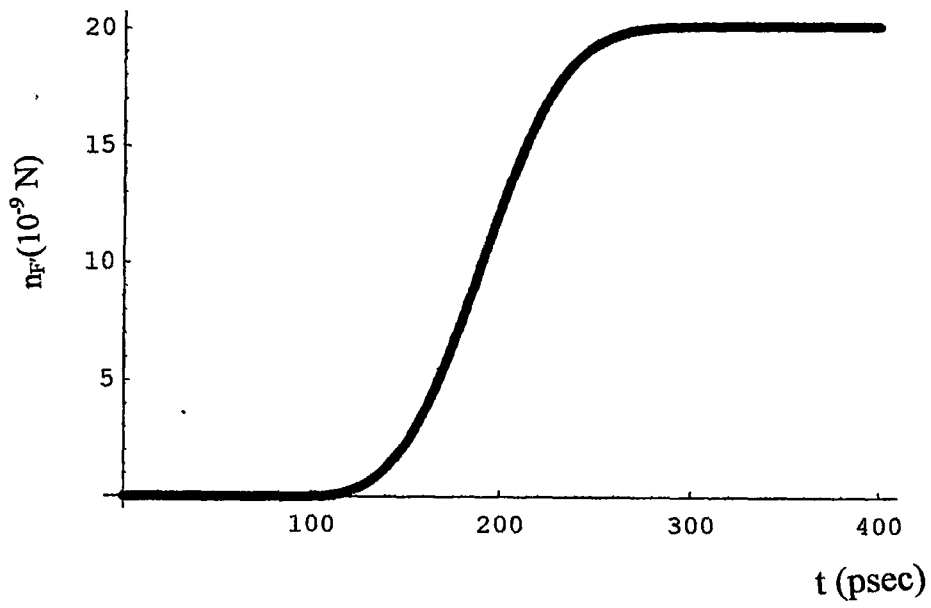


**Figure 5.22** Density of ionized F-center  $n_F$ , with multiphoton-assisted-avalanche model.

# CHAPTER 6

## RESULTS AND CONCLUSIONS

Many defects are unstable entities and rapidly change to new equilibrium charge states or rearrange in the lattice. For a full understanding of the processes involved it is necessary to study many defects at the moment of formation. For example on irradiation of an alkali halide we expect to form the two simplest centers of a halogen vacancy (F-center) and a halogen interstitial center (H-center). The F-and H-centers are highly unstable at normal temperatures, so most measurements reveal some later and more complex stage of development.

Optical absorption measurements are relatively simple to make but none the less they give considerable information on the symmetry, concentrations and interactions of the various centers and because the transition energies produce optical absorption bands in different spectral regions, the properties of different defects may be resolved.

In this work, we studied the multiphoton absorption and electron avalanche formation in the phenomenon of laser damage of transparent solids, and concentration of primary defects. The damage mechanism active in NaCl at 532 nm had not been unequivocally assigned to be either avalanche or multiphoton.

In a review of literature in 1988, Jones et al.[9] obtained the four-photon cross section by experimentally and obtained the conduction band free-carrier concentration

with  $\sigma^{(4)} = 2 \times 10^{-113} \text{ cm}^8 \text{ sec}^3$  using multiphoton-polaron-defect heating model. We have used the multiphoton-polaron-defect heating model and multiphoton-assisted-defect heating model  $\sigma^{(4)} = 2 \times 10^{-113} \text{ cm}^8 \text{ sec}^3$  and  $\sigma^{(4)} = 1.5 \times 10^{-114} \text{ cm}^8 \text{ sec}^3$  respectively. We have obtained primary defects mentioned above. The comparison of the conduction band free carrier concentration,  $n_c$ , obtained with multiphoton-polaron-defect model by Jones [9] is shown in Figure 4.3 and by us (Figure 5.1) indicates a similar behavior but also shows that there is a factorial difference between them. The results obtained from this work are generally in agreement with the literature.

Figure 5.5 shows change in the concentration of the  $V_{K3^-}$  center with respect to time. As it has been seen from the Figure of  $V_{K3^-}$  center, density increases exponentially up to 250 psec; then it seems to level off. There may be two possible explanation for this behavior ;  $V_{K3^-}$  center may consist of deep traps so that laser excitation may not be high enough to excite  $V_{K3^-}$  center. This trap center does not convert to other centers. Also ionized F-center  $n_F$  shows the same behavior with  $V_{K3^-}$  center.

We have to mention that we could not find any results related to  $V_{K3^-}$  center density in literature. Therefore it was not possible to compare our results with literature.

We have also solved the kinetic equations for three values of peak flux  $F_p$ , corresponding to  $\sigma^{(4)} = 2 \times 10^{-113} \text{ cm}^8 \text{ sec}^3$  and  $\sigma^{(4)} = 3 \times 10^{-113} \text{ cm}^8 \text{ sec}^3$  to obtained concentration of the free carrier density. As seen from Figures 5.11, 5.12 changing the four-photon cross section  $\sigma^{(4)}$ , value for the same  $F_p$ 's made very slight changes on the concentration of free carrier density  $n_c$ . However changing  $F_p$ 's values for the same  $\sigma^{(4)}$ , made very significant changes. As  $F_p$  values increased the peak value of  $n_c$  largely increased.

We have solved the rate equations also using the multiphoton-assisted-avalanche-defect heating model. The concentration of species Figures 5.13 to 5.22 are very low due to this model. The crystal may be damaged.

The conduction band free carrier density,  $n_c$ ,  $V_{K3}$ -center, ionized F-center,  $n_F$ , in model multiphoton-assisted-avalanche-defect heating model show the same behavior as  $V_{K3}$ -center in multiphoton-polaron-defect-heating model.

The concentration of free hole density,  $p$ ,  $V_{K1}$ -,  $V_{K2}$ -center are very low as seen in Figures 5.14, 5.15, 5.16 respectively.

The concentration of STEs and  $n_F$  are zero as seen in Figure 5.18, 5.19, 5.20, 5.21 respectively. Due to heating the crystal may be damaged.

As mentioned in Chapter 5 , the STE states contribute negligibly to energy absorption. But it is necessary to include them, however, at high temperature, F-center are formed through the  $S_3$  STE state.

The model parameters are not known exactly, so that we could have easily decided to vary them and obtain an enormous amount of output for the various parameter values.

Results can be carried over to the study of the more important materials of high-power laser components such as  $CaF_2$ ,  $Mg F_2$ , which have band gaps and defect properties similar to the alkali halides.

## LIST OF REFERENCES

- [1] E. Yablonovitch and N. Bloembergen, Phys. Rev. Lett. 29, 907(1972).
- [2] N. Bloembergen, IEEE J. Quantum Electronics QE-10, 375(1974).
- [3] W.L.Smith, Opt.Eng.17, 489(1978).
- [4] P.Braunlich, A.Schimd, and P.Kelly, Appl. Phys. Lett. 26, 150(1975).
- [5] A.Schimd, P.Braunlich, and P.Kelly, Phy.Rev. B 16, 4569(1977).
- [6] P. Kelly, A. Schimd, and P.Braunlich, Phys. Rev. B 20, 815(1979).
- [7] B.G. Gorshkov, Yu.K. Danileiko, A.S. Epifanov, V.A. Lobachev, A.A. Manenkov, and A.V. Sidorin, Sov.Phys. JETP 43, 309(1979).
- [8] W.L. Smith, J.H. Bechtel, N. Bloembergen, Phy. Rev. B 15, 4039(1977).
- [9] S.C. Jones, A.H. Fischer and P. Braunlich, and Kelly, Phy.Rev. B 37, 755(1988).
- [10] S. Brawer, Phys. Rev. B 20, 3422(1979).
- [11] P. Horn, P.Braunlich, and A. Schmid, J. Opt. Soc. Am. B 2, 1095(1985).
- [12] G. Brost, P. Braunlich, and P. Kelly, Phy. Rev. B 30, 4675(1984).
- [13] J.N. Bradford, R.T. Williams, and W.L. Faust Phys. Rev. Lett. 35, 300(1975).
- [14] Y. Suzuki, and M. Hirai, J. Phys.Soc.Japan 43, 1679(1977).
- [15] R.T. Williams, J.N. Bradford and W.L. Faust Phys. Rev. B 18, 7038(1978).

- [16] R.T. Williams, and M.N. Kabler, Phys. Rev. B 9, N4, 1897(1974).
- [17] W.B. Fowler, In Physics of Color Centers, edited by W.B. Fowler (Academic, New York, 1968).
- [18] N. Itoh, Adv. Phys. 31, 491(1981).
- [19] C. B. Lushchick, I.K. Vitol and M.A. Elango, Usp. Fiz. Navk. 122, 223(1977).
- [20] R.T. Williams, B.B. Craig, and W.L. Faust, Phys.Rev.Lett. 52, N19, 1709(1984).
- [21] E.W. Von Stryland, M.J. Soileau, A.L. Smirl, and W.E. Williams, Phys. Rev. B 23, 2146(1981).
- [22] G.W. Bryant, P.Kelly, D.Ritchie, P. Braunlich, and A. Schmid, Phys.Rev. B 2587(1982).
- [23] P.Horn, A. Schmid, and P. Braunlich, IEEE J. Quantum Electronics, QE-19, No. 7, 1169(1983).
- [24] V.S. Dneprovskii, D.N. Klyshko, and A.N. Penin, Sov.Phys. JETP Lett. 3, 251(1966).
- [25] G.I. Aseev, M.L. Kats, and V.K. Nikol'skii, Sov.Phys. JETP Lett. 8, 103 (1968).
- [26] I.M. Catalano, A.Cingolani, and A. Minatra, Phys.Rev. B 5, 1629(1972).
- [27] R.T. Williams, P.H. Klein, and C.L. Marquardt, NBS Special Publication 509, 481(1977).
- [28] R.Chen, S.W.S. McKeever, and S.A.Durrani, Phys.Rev. B 24, 4931(1981).
- [29] B.G. Gorshkov, Yu.K. Danileiko, A.S. Epifanov, V.A. Lobachev, A.A.

- Manenkov, and A.V. Sidorin, Sov. Phys. JETP 45, 612(1977).
- [30] P. Braunlich, G Brost, A.Schmid, and P. Kelly, IEEE J. Quantum Electronics  
Vol. QE-17, No:10, 2034(1981).
- [31] R.T. Casper, S.C. Jones, and P. Braunlich, Nuclear Ins. and methods in Phys.  
Research B, 46231(1990).
- [32] P. Kelly, S.C. Jones, X.A. Shen, L. Simpson, P. Braunlich, and R.T. Casper  
Phys. Rev. B 47, 11370(1990).
- [33] K. Soda, and N.Itoh Journal of the Physical Society of Japan Vol. 50, No:12,  
3988(1981).
- [34] X.A. Shen, S.C. Jones, and P. Braunlich, Phys. Rev. B 36, 2831(1987).
- [35] X.A. Shen, P. Braunlich, S.C. Jones, and P. Kelly, Phys. Rev. B 38, 3494(1988).
- [36] B.G. Gorshkov, L.M. Dorozhkin, A.S. Epifanov, A.A. Manenkov, and A.A.  
Panov, Sov. JETP 61, 12(1985).
- [37] R. Leonelli and J.L. Brebner Phys. Rev. B 33, 8649(1986).
- [38] A.S. Epifanov, A.A. Manenkov, and A.M. Prokhorov, Sov.Phys. JETP  
43,397(1976).
- [39] B.G. Gorshkov, A.S. Epifanov, and A.A. Manenkov, Sov.Phys. JETP  
49, 309(1979).
- [40] A.S. Epifanov, IEEE J. Quantum Electronics Vol. QE-17, No:10, 2018(1981).



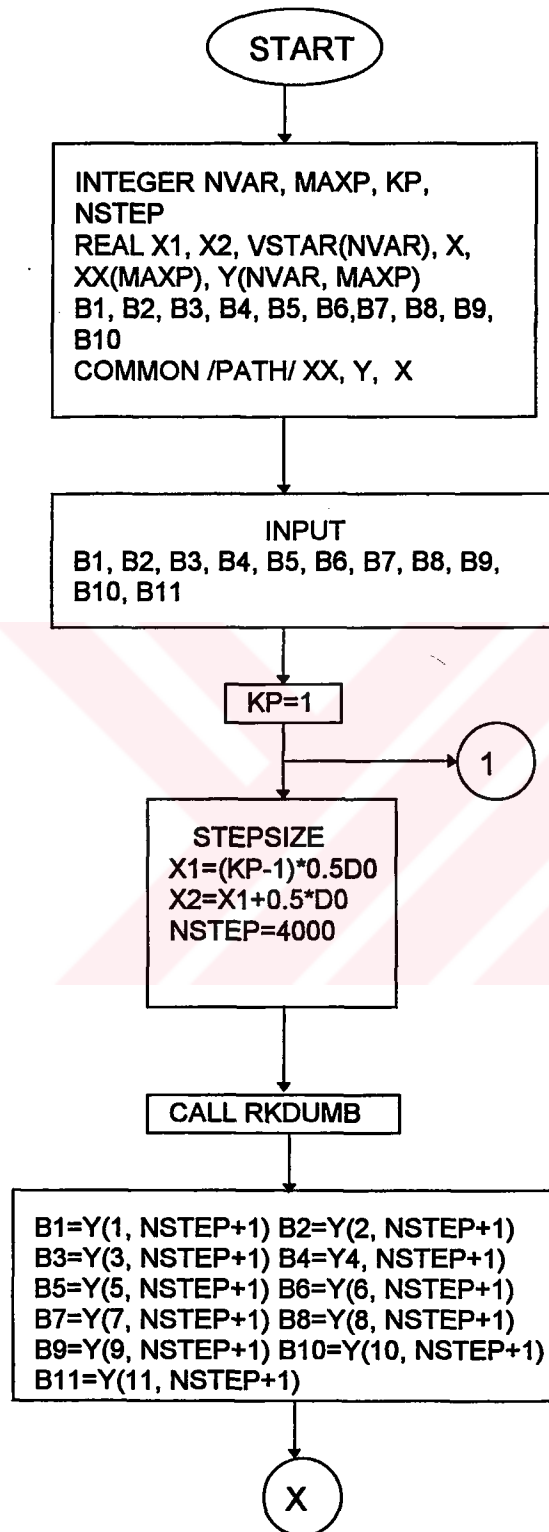
- [41] X.A. Shen, S.C. Jones, and P. Braunlich, Phys. Rev. Lett. 62, 2711(1989).
- [42] S.T. Wu, and M. Bass, Appl. Phys. Lett. 39, 948(1981).
- [42] V.Nathan, A.H. Guenther, and S.S. Mitra, J. Opt. Soc. Am. B 2, 294(1985).
- [43] M. Sparks, D.L. Mills, R. Waren, T. Holstein, A.A. Maradudin, L.J. Sham, E. Loh, and D.F.King, Phys.Rev. B 24, 3519(1981).
- [44] R.T. Williams, K.S. Song, W.L. Faust, and C.H. Leung, Phys. Rev. B 33, 7232(1986).
- [45] S. Wakita, Y. Suzuki, H. Ohtami, S. Tagowa, and M. Hirai, J. Phys Soc.Jpn.50,3378(1981).

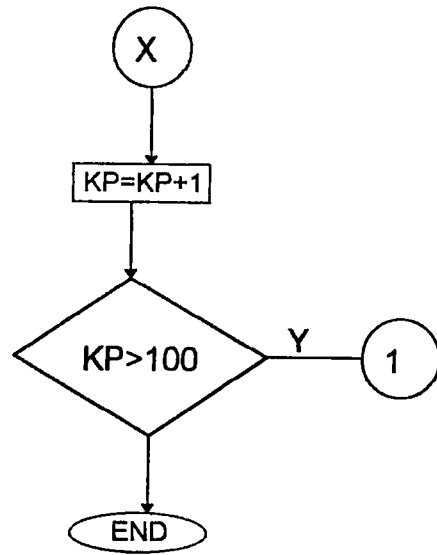


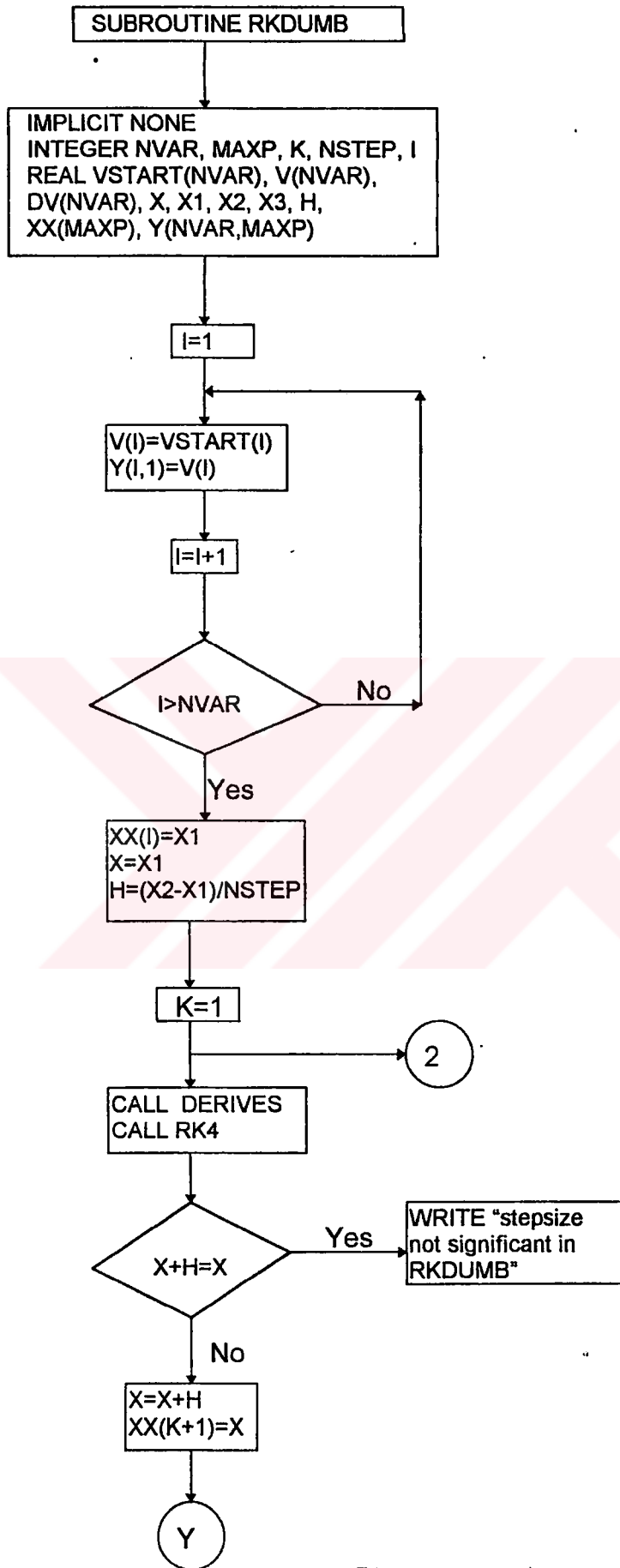


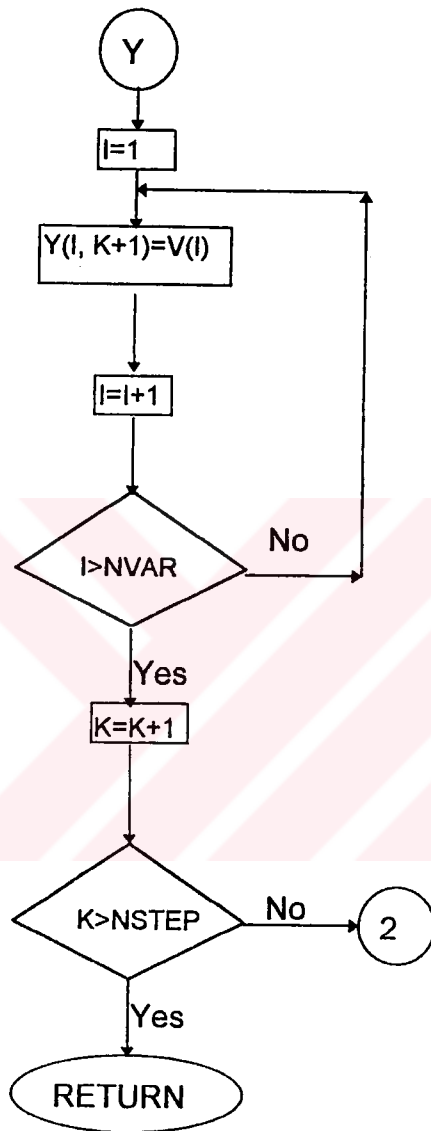
**APPENDIX**

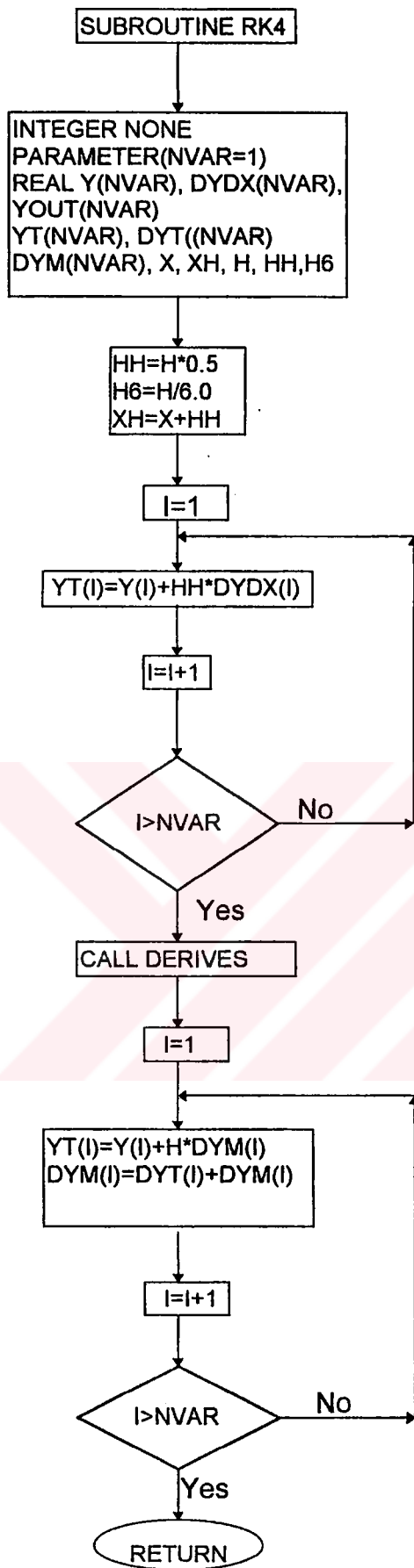
# FLOW CHART OF RK4 TO SOLVE DIFFERENTIAL EQUATIONS

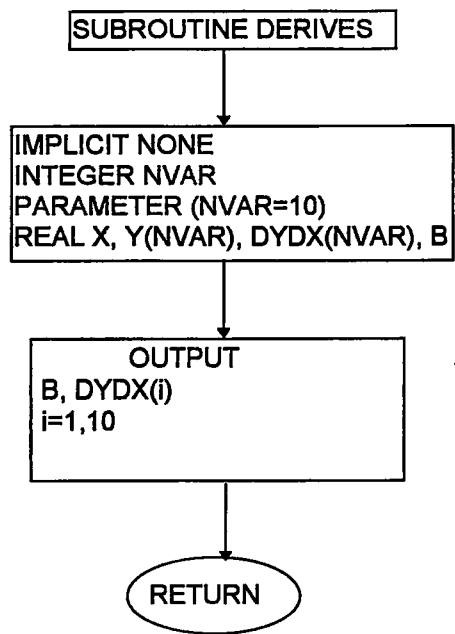














## **CIRRICULUM VITAE**

The author was born in Birecik, Şanlıurfa on October, 1964. She graduated from the primary, secondary, and high schools in Gaziantep, in 1975, 1978, 1981 respectively. She received the B. S. degree from physics engineering department at Gaziantep Engineering Faculty of Middle East Technical University, in 1988. She started to work as research assistant in Department of Physics Engineering of University of Gaziantep in 1989. She also received the M. Sc. degree from the Department of Physics Engineering of the University of Gaziantep, in 1991. In 1993 she was accepted to the Ph.D. program in Engineering Faculty of University of Gaziantep.

She is married and has a son.